DEFLECTION AND VIBRATION ANALYSIS OF A FLEX FAN BLADE

DEFLECTION AND VIBRATION ANALYSIS OF A FLEX FAN BLADE USING THE FINITE ELEMENT TECHNIQUE

by

DEVENDRA M. GOSSAIN, B.TECH. (HONS.)

A THESIS
SUBMITTED TO THE SCHOOL OF GRADUATE STUDIES
IN PARTIAL FULFILMENT OF THE REQUIREMENTS
FOR THE DEGREE
MASTER OF ENGINEERING

McMASTER UNIVERSITY
FEBRUARY 1972.

MASTER OF ENGINEERING
(Mechanical Engineering)

McMASTER UNIVERSITY
Hamilton, Ontario.

TITLE: Deflection and Vibration Analysis of a Flex Fan Blade Using the Finite Element Technique.

AUTHOR: Devendra M. Gossain, B.Tech. (Hons.)
(Indian Institute of Technology, Kharagpur, India.)

SUPERVISOR: Professor M.A. Dokainish

NUMBER OF PAGES: ix, 100

SCOPE AND CONTENTS:

A flex-fan has flexible blades which undergo large deformation under centrifugal forces to give the desired air-flow and power-consumption characteristics with speed. The finite element technique has been used to obtain the deflected shape of the blade of such a fan used for automobile radiator cooling. The natural frequencies of vibration are also evaluated at different speeds, up to 5,000 rpm. A partially conforming deflection function has been used in the analysis. The blade has been treated as a thin shell, idealized as an assembly of thin flat triangular elements.

ACKNOWLEDGEMENTS

The author is pleased to record his thanks to Professor Dokainish for suggesting the problem for investigation, his guidance at various stages, and his patience at times of exasperating computational and de-bugging difficulties.

Thanks are also due to Miss Sheelagh Swords for an intelligent typing of the manuscript.

The National Research Council of Canada Grant No. A-2726 used for this investigation is also gratefully acknowledged.

- - - - - - - - - - - - - - - - -

TABLE OF CONTENTS

		PAGE NO.
CHAPTER 1:	INTRODUCTION	
1.1	Introduction	1
1.2	The Flex Fan	2
1.3	Principle of Operation	3
1.4	Design Features of the Fan	4
1.5	Deflection and Vibration Analysis	4
CHAPTER 2:	LITERATURE SURVEY	
2.1	Flex Fans	6
2.2	The Finite-Element Technique	6
CHAPTER 3:	FINITE ELEMENT FORMULATION	
3.1	Theory	12
3.2	Idealization of the Fan Blade	17
3.3	Boundary Conditions	18
3.4	Procedure for Solution	20
3.5	The Stiffness Matrix	21
3.6	Transformation to Global Co-ordinates	33
3.7	Centrifugal Stiffness Matrix	37
3.8	Centrifugal Loading	39
3.9	Nodal Equivalent of the Distributed Centrifugal Force.	42
3.10	Calculation of the Deflections	46
3.11	The Vibration Problem	46
3.12	The Stiffness-Correction Matrix	49
3.13	The Mass Matrix	51

PAGE NO.

CHAPTER 4: RESULTS AND DISCUSSION

4.1 Deflection 55

4.2 Natural Frequencies 58

4.3 Discussion 63

FIGURES 64

REFERENCES 79

APPENDICES

I - Elements of [Z] matrix 84

II - Derivation of the Inertia Forces 87

III - Elements of [NF] matrix 90

IV - Elements of [NQ] matrix 93

V - Flow Chart for the Computer Programme for Deflection 97

VI - Flow Chart for the Computer Programme for Natural Frequencies 99

VII - Modification Required to Suit "Variable" Boundary Condition. 100

LIST OF SYMBOLS vii

LIST OF SYMBOLS

E	-	Elastic modulus of the material of the blade.
μ	-	Poisson's ratio of the material of the blade.
t	-	Thickness of the blade.
ρ	-	Density of the material of the blade.
g	-	Acceleration due to gravity.
θ	-	Angle made by the post with the axis of rotation.
Ω	-	Speed of rotation of the fan
w	-	Natural frequency of vibration.
x, y, z	-	Global co-ordinates.
x', y', z'	-	Local co-ordinates of the element.
i, j, k	-	Nodes of an element.
u', v', w'	-	Displacements in the direction of x', y' & z' axes in local co-ordinates.
u, v, w	-	Displacements in the direction of x, y & z axes in global co-ordinates.
$\varepsilon_{x'}, \varepsilon_{y'}$	-	Normal strains in the direction of x' and y' respectively.
$\varepsilon_{x'y'}$	-	Shear Strain in the plane x'y'.
$\sigma_{x'}, \sigma_{y'}$	-	Normal stresses in the direction of x' and y' respectively.
$\tau_{x'y'}$	-	Shear stress in the plane x'y'
ℓ_x, m_x, n_x	-	Direction cosines of x' axis.
ℓ_y, m_y, n_y	-	Direction cosines of y' axis.
ℓ_z, m_z, n_z	-	Direction cosines of z' axis.
$F_{x'}, F_{y'}, F_{z'}$	-	Forces in the direction of x', y' & z' axes respectively.
F_x, F_y, F_z	-	Forces in the direction of x, y and z axes respectively.

Matrices

$[K'_p]^e$ - In-plane stiffness matrix of an element in local co-ordinates.

$[K'_b]^e$ - Bending stiffness matrix of an element in local co-ordinates.

$[K']^e$ - Total stiffness matrix of an element in local co-ordinates.

$[\lambda]$ - 3 x 3 matrix of direction cosines.

$[K]^e$ - Total stiffness matrix of an element in global co-ordinates.

$[K'_{cs}]$ - Centrifugal stiffness matrix of an element in local co-ordinates.

$\{F'_{15}\}$ - Vector of nodal equivalent forces for an element in local co-ordinates.

$\{F\}^e$ - Vector of nodal equivalent forces for an element in global co-ordinates.

$[K]^s$ - Stiffness matrix of the system in global co-ordinates.

$\{F\}^s$ - Vector of nodal equivalent forces for the system.

$[K'_{sc}]^e$ - Stiffness Correction matrix of an element in local co-ordinates.

$[K_{sc}]^s$ - Stiffness Correction matrix for the system.

$[m'_p]^e$ - In-plane mass matrix of an element in local co-ordinates.

$[m'_b]^e$ - Bending mass matrix of an element in local co-ordinates.

$[m']^e$ - Total mass matrix of an element in local co-ordinates.

$[m]^e$ - Total mass matrix of an element in global co-ordinates.

$[m]^s$ - Mass matrix of the system.

Superscripts

'	- The quantity referred to in local axes (x', y', z'). When this superscript is dropped, the quantity referred to in global axes (x, y, z).
*	Virtual displacement.
°	First derivative with respect to time (e.g. $\dot{u}$, $\dot{v}$ etc.).
°°	Second derivative with respect to time (e.g. $\ddot{u}$, $\ddot{v}$ etc.).
-1	Inverse of matrix.
T	Transpose of matrix.

Subscripts

eq	Equivalent nodal forces corresponding to distributed loads.
i,j,k	Value of the quantity at nodes i, j and k.

CHAPTER 1

1.1 Introduction

All internal combustion engines require cooling for satisfactory performance. In power units where the speed of the engine and its load vary considerably - the most common example of such a unit being the automobile engine - it is essential to control cooling to maintain the engine temperature within a close range to ensure minimum friction and rate of cylinder wear. Figure 1.1 shows the average friction loss at different cylinder temperatures for two typical engines.

The design of cooling fans for modern automobiles is made more difficult by the introduction of additional factors - rising cooling loads in today's engines, styling trends that reduce radiator space, heat loads from air conditioning condensers, and the necessity to keep fan horsepower and noise at low levels.

The control of cooling has been achieved by different methods. The two basic approaches have been:

1) throttling the air either at the inlet or at the outlet to the fan

2) varying the fan rotational speed to get the required amount of air.

The second approach has been more popular for automobiles. At high

vehicle speed the natural air flow can be utilized for cooling. Hence, the fan rotational speed can be reduced as the vehicle speed increases, resulting in considerable saving in power, since air flow through the fan is proportional to the speed of rotation and power input to the fan is proportional to the third power of the speed of rotation.

The popular method of speed variation has been the introduction of a variable speed clutch between the engine and the fan. The clutch may be electro-magnetic, mechanical or viscous. The viscous clutch is most widely used because of its simplicity of operation. The speed ratio in the clutch is varied by varying the amount of the circulating fluid in the clutch. The clutch is actuated by a temperature sensitive control. This control, by sensing the temperatures of the cooling system, varies the fan-to-engine speed ratio according to the actual cooling requirements. The characteristics of a typical temperature modulated clutch and fan are shown in Figure 1.2 and Figure 1.3.

1.2 The Flex Fan

A new type of cooling fan in which the blades are flexible (hereafter referred to as a "flex-fan") has recently been developed. The blades are made very thin so that the pitch of the blades decreases with increasing fan speed. This reduces the air-flow and power consumption and eliminates the need of a viscous clutch. The design details and research work done to develop this fan have been reported in detail by Cassidy & White [1]*.

*Numbers in square brackets indicate references at the end of the thesis.

Such a fan has the advantages of simple construction, reduced number of parts in the fan assembly (due to elimination of the clutch), lower initial cost, and less maintenance attention.

1.3 Principle of Operation

The principle of operation can be explained by considering one blade of the fan as shown in Figure 1.4. One edge of the blade is rivetted to a rigid radial post. The rotation of the fan causes centrifugal force to act on the blade. The centrifugal force F on a small element acts radially outwards from the axis of rotation and can be resolved into two orthogonal components, F_x and F_y, in the plane normal to the axis of rotation. The component F_x can again be resolved into a component F_A in the plane of the element and a component F_p perpendicular to it. The component F_p causes bending while the components F_A and F_y cause in-plane stretching.

Every element on the blade, thus, has a component of the centrifugal force acting in the direction of the normal, tending to bend the blade and thus decrease its curvature. The magnitude of the force depends upon the position of the element on the blade and the angle between the post and the axis of rotation. The loading due to the component F_p is resisted by the elastic forces within the blade. At every rotational speed, an equilibrium is reached between the centrifugal loading and the internal reaction of the blade. Since the curvature of the blade decreases with increasing speed, the air-flow through the fan is reduced.

1.4 Design Features of the Fan

A typical flex-fan, shown in Plate I, has five blades, each made of spring steel sheet of thickness 0.020". The profile of the blade at zero speed is a circular arc. The blade, therefore, is a segment of a circular cylinder. One edge of the blade is rivetted to the rigid post. The post is radial but inclined at an angle to the axis of rotation. The blade also has a "lip" underneath as shown in Figure 1.5. This lip prevents large amplitude vibrations of the blade and also makes it stiffer with increasing deflection since the blade rolls on the "lip" as it deflects. The effect of the lip is similar to that of a variable boundary condition of a cantilever beam - as the beam deflects its effective length becomes shorter and hence its natural frequency increases (Fig. 3.2). The large amplitude vibrations are thus prevented when the fan is excited at one of its natural frequencies.

The parameters that the fan designer can vary to get the desired performance over the complete speed range include the blade thickness, width and length of the blade, post angle and distance of the blade from the centre of the fan.

1.5 Deflection and Vibration Analysis

Due to the complex nature of loading on the fan, the shape of the blade at different rotational speeds cannot be easily determined analytically. The present study uses the finite-element technique to determine the deflected shape and the natural frequencies of the blade at different rotational speeds.

Information regarding the shape of the blade at different speeds can be used to predict the air-flow from the fan. In the present study, the deflected shape of the blade has been determined up to 5000 rpm.

The vibration characteristics of the fan also change with speed due to the change in blade shape and due to the presence of in-plane stresses introduced by the centrifugal loading. The knowledge of the natural frequencies can be useful in predicting the effect of excitation by the high-order firing frequencies of the engine. The first five natural frequencies have been determined at different speeds, up to 5000 rpm.

The finite-element analysis has been performed by considering the blade as a shell and approximating it as an assembly of flat triangular elements.

The air-loading on the blade has been neglected since the analysis of this loading and its effect on blade vibrations is beyond the scope of this thesis.

CHAPTER 2

LITERATURE SURVEY

2.1 Flex-Fans

A discussion of the necessity of cooling-control in automotive engines and the details of the various methods used for controlling the speed of radiator fans can be found in many standard texts on automobile engine design. A good treatment is given by Mackerle [2]. Brabetz [3] has discussed the importance of cooling control.

The idea of using fans with flexible blades for automotive cooling is quite old. Paton [4] got a patent for such a fan in 1936. Senn [5] patented a turbine rotor with flexible blades in 1948. However, such a fan was not successfully used till quite recently. In 1963, Bosh [6] patented a variable-pitch fan blade. In 1966, the development of a successful fan with flexible blades (called the "flex-fan") was reported by Ford Motor Co. The details of the research, design and testing done for the fan before it was released for regular use, were published by Cassidy and White [1]. They determined the air-flow characteristics of the fan experimentally for different models.

2.2 The Finite-Element Technique

The matrix method for analysis of conventional engineering structures, like frames, is well known. Such a structure may be

visualized as an assemblage of structural elements (beams) inter-connected at a discrete number of nodal points. If the force-displacement relationships for the individual beam elements are known, it is possible, by using the well known techniques of structural analysis [7], to derive the properties of the complete structure and to study its behaviour.

In a continuous structure, like a plate or a shell, the division of the elastic medium into elements poses a problem in numerical solution since the number of inter-connecting points between the elements is infinite. However, the concept of "finite-elements", originally introduced by Turner et al [8], overcomes this difficulty by assuming the real continuum to be divided into elements inter-connected only at a finite number of nodal points. Forces, representative of the distributed stresses and discrete forces actually acting on the element boundaries, are introduced at the nodes. The nodal force-displacement relationships are obtained by assuming displacement shapes within the element in terms of the nodal displacements. This idealisation reduces the problem to that of a conventional structural type, well amenable to numerical solution.

The success of the finite-element technique for two-dimensional elastic problems was demonstrated by Turner et al [8] and Clough [9]. Turner et al used a triangular element with six degrees of freedom (two per node, in-plane) and a linear assumed displacement variation. An improved triangular element was suggested by Veubeke [10] and Argyris [11]. This triangular element has six nodes.

For plate bending, Melosh [12] presented a fourth-degree polynomial for a rectangular element. A satisfactory sixteen-degrees-of-freedom rectangular element was developed by Bogner, Fox and Schmit [13], Butlin and Leckie [14] and later by Mason [15].

A deflection function for triangular plate elements in bending, with three degrees of freedom per node, was introduced by Tocher [16]. This deflection function is of the form:

$$U_z = C_1+C_2x+C_3y+C_4x^2+C_5xy+C_6y^2+C_7x^3+C_8(x^2y+xy^2)+C_9y^3$$

where

C_1, C_2....C_9 are constants and U_z is the deflection in z-direction.

Gallagher [17] suggested the function:

$$U_z = C_1+C_2x+C_3y+C_4x^2+C_5xy+C_6y^2+C_7x^3+C_8xy^2+C_9y^3$$

This function does not preserve the symmetry in x and y as Tocher's function does.

Rawtani [18] used the function:

$$U_z = C_1+C_2x+C_3y+C_4x^2+C_5xy+C_6y^2+C_7x^3+C_8x^2y+C_9y^3$$

This function is partially conforming since the displacement and the slopes along one edge of the element can be made conforming by suitable choice of the co-ordinate axis.

A discussion of different forms of deflection functions employed for calculation of triangular plate element stiffness is given by Clough and Tocher [19] and Bazley et al [26].

The Rectangular plate elements in bending have been developed by Gallagher et al [21] and Melosh [22]. Quadrilateral elements have also been developed by Zienkiewicz and Cheung [23], Dawe [24] and Argyris [25].

The elements mentioned above have the drawback that the displacement functions are not completely conforming, that is, displacements, slopes, etc. along the common boundaries between elements are not completely compatible resulting in "kinks" or discontinuities along these boundaries. In most cases, however, the results obtained by using these functions converge with increasing mesh size.

The development of shape functions, for lateral displacements, which satisfy complete continuity requirements between elements has been the object of recent research. Bazley et al [20] and Clough et al [19] have reported successful use of functions in which linear variations of slope along the boundaries is imposed. This condition implies that displacement function cannot be defined by a single polynomial throughout the element. Cowper et al [26] and Bell [27] have independently reported a "high precision" triangular element with 18 degrees of freedom. It makes use of six deflection parameters at each vertex, namely the transverse deflection and its first and second derivatives. The displacement function for the element is taken as a quintic polynomial. This element is reported to be more suitable for dynamic investigations.

Considerable progress has been made in the past few years in applying the finite element method to the analysis of shell structures.

The initial work in this area was devoted to shells of revolution in which closed rings or conical shell segments were used to model the complete structures. Much of this work has been reviewed by Jones and Strome [28]. The use of such elements is limited since they can be applied only to shells of revolution with cylindrical or conical shapes.

Attempts to develop a finite element method for general shell structures have generally followed two different courses. In the first approach, the shell is replaced by an assemblage of flat plate elements which are either triangular or quadrilateral in shape. Each plate element is connected at the nodes to those surrounding it, and undergoes both bending and stretching deformations. This approach has been successfully used for general shell shapes by Zienkiewicz and Cheung [29] and Clough and Johnson [30]. However, the method has the disadvantage that there is no coupling between bending and stretching within each element and, consequently, a large number of elements have to be used to achieve accuracy. The second approach is to develop curved shell elements that permit closer geometric representation of a shell structure. Such an approach has been followed with good results for the case of cylindrical shells where cylindrical elements are adequate. Successful cylindrical shell elements have been developed by Bogner et al [31], Cantin and Clough [32] and Olson and Lindberg [33]. Research on rectangular and quadrilateral elements for general shells has been done by Connor and Brebbia [34] and Gallaghar [17]. Shallow shell triangular elements have been developed by Utku and Melosh [35], Strickland and Loden [36] and Bonnes et al [37]. Most recently, Cowper et al [38] developed a

shallow shell triangular element based on an eighteen-degrees-of-freedom triangular plate element. The final shell element has 36 degrees of freedom.

The large-displacement problems can also be handled by finite-element technique using an iterative approach consisting of small linear steps. The process can be simplified by formation of "geometric" stiffness matrix as suggested by Argyris [25] when the strain within an element is small and can be ignored.

CHAPTER 3

FINITE ELEMENT FORMULATION

3.1 Theory

The Finite element technique involves formulation of a discrete-element mathematical model equivalent to the actual continuous structure. This model is necessary in order to have a system with a finite number of degrees of freedom upon which the matrix algebra operations can be performed. The details and the theory of the method are discussed extensively in the texts by Zienkiewicz [29], Przemieniecki [39] and Rubenstein [46]. Only a brief outline of the theory is, therefore, presented here.

The continuum of the structure is separated by imaginary lines or surfaces into a number of "finite-elements". The elements are assumed to be inter-connected at a discrete number of nodal points situated on their boundaries. The generalized displacements (lateral displacement, rotation etc.) are the basic unknown parameters of the problem.

The properties of the whole structure are built from the elastic and inertia properties of the constituent discrete elements. The first step in determining the properties of the element is to assume that the interior displacement vector $\{f\}$ is expressible in terms of the nodal displacement vector $\{\delta\}^e$ by the matrix equation

$$\{f\} = [N]\ \{\delta\}^e \qquad (3.1)$$

For continuously attached elements, idealized as elements with discrete nodal points, [N] is determined by assuming the form of displacement distribution - specifically, a linear combination of different continuous functions with arbitrary multiplying constants. The number of constants is equal to the number of discrete displacements - these constants can therefore be determined in terms of the nodal displacements.

With the displacements known at all points within the element the strain vector $\{\varepsilon\}$ at any point can be determined. This will always result in a relationship which can be written as:

$$\{\varepsilon\} = [B] \{\delta\}^e \tag{3.2}$$

If the elastic behaviour of the material is known, the stress vector $\{\sigma\}$ can be determined from the relationship:

$$\{\sigma\} = [D] \{\varepsilon\} \tag{3.3}$$

where [D] is an elasticity matrix containing the appropriate material properties. Substituting eq. (3.2) in eq. (3.3), we get:

$$\{\sigma\} = [D] [B] \{\delta\}^e \tag{3.3a}$$

The stiffness matrix of the element can be obtained by applying the principal of virtual work. Let $\{\delta^*\}^e$ be a virtual displacement at the nodes. This results in displacements $\{f^*\}^e$ and strains $\{\varepsilon^*\}$ within the element given by:

$$\{f^*\} = [N] \{\delta^*\}^e$$

and

$$\{\varepsilon^*\} = [B] \{\delta^*\}^e$$

The work done by the nodal forces is given by $(\{\delta^*\}^e)^T.\{F\}^e$. Similarly, the internal work done, per unit volume, by the stresses in the element is given by $\{\varepsilon^*\}^T \{\sigma\}$. Equating the total internal work done, obtained by integrating over the volume of the element, with the work done by the nodal forces, we have:

$$(\{\delta^*\}^e)^T (\{F\})^e = \int \{\varepsilon^*\}^T \{\sigma\} \, d(Vol)$$

Using eq. (3.2) and eq. (3.3a) we get:

$$(\{\delta^*\}^e)^T \{F\}^e = (\{\delta^*\}^e)^T \left(\int [B]^T [D][B] d(Vol)\right)\{\delta\}^e$$

As this relation is valid for any value of the virtual displacement, the equality of multipliers must exist. Hence:

$$\{F\}^e = \left(\int [B]^T [D][B] d(Vol)\right)\{\delta\}^e$$

This equation can be written in the form

$$\{F\}^e = [K]^e \{\delta\}^e$$

relating nodal forces with nodal displacements. The matrix $[K]^e$ is called the stiffness matrix of the element and is given by:

$$[K]^e = \int [B]^T [D][B] d(Vol) \qquad (3.4)$$

The stiffness matrix of the complete structure can be formed by combining the stiffness matrices of all the elements.

If the co-ordinate system used for the element is the same as the global or system co-ordinates, the stiffness matrices can be directly assembled to get the system stiffness matrix $[K]^s$.

If the co-ordinate system used for the element (called the "local co-ordinate system") is different from the global co-ordinates, as is

usually done for programming convenience, element stiffness matrix has to be transformed before assembly. The local and global co-ordinates are related by the transformation:

$$\{\delta\}^e_l = [L]\ \{\delta\}^e_g \tag{3.5}$$

where the subscripts l and g stand for local and global co-ordinates respectively, and [L] is the matrix of direction cosines between the local and the global axes.

The element stiffness matrix in the global co-ordinates, $[K]^e_g$, is obtained by the relation:

$$[K]^e_g = [L^{-1}]\ [K]^e_l\ [L] \tag{3.6}$$

As the transformation matrix is orthogonal

$$[L^{-1}] = [L]^T$$

and

$$[K]^e_g = [L]^T [K]^e_l\ [L] \tag{3.7}$$

The nodal forces {P} and nodal displacements {U} for the complete structure are now related by the system stiffness matrix $[K]^s$ as

$$\{P\} = [K]^s\ \{U\} \tag{3.8}$$

However, the stiffness matrix obtained thus is singular; that is, $[K]^s$ cannot be inverted to find the nodal displacements from equation (3.8).

Vector {P} in eq. (3.8) includes the reactions and the applied loads. The singularity of $[K]^s$ is due to the inter-dependence of the reactions and the applied forces. From the considerations of overall equilibrium, equations corresponding to the rigid body degrees-of-freedom of the structure relate the reactions to applied forces. The singularity

of $[K]^s$ is removed by considering the boundary conditions on the structure and deleting the rows and columns corresponding to the rigid body degrees of freedom, and the additional displacements constrained to be zero by the boundary conditions. The stiffness matrix $[K]^s$ can now be inverted to obtain the displacements from equation (3.8) if the applied forces are known.

In the above discussion, the forces are assumed to be applied at the nodes. If distributed loads are acting on the element, statically equivalent nodal forces may be found for the distributed loads before carrying out the analysis. The distributed loads $\{p\}$ are defined as those acting on a unit volume of material within the element with directions corresponding to those of the displacements $\{f\}$ at that point.

The nodal equivalent forces may be found by imposing an arbitrary (virtual) nodal displacement and by equating the external and internal work done by the various forces and stresses during that displacement. This gives the nodal equivalent forces for the element $\{F\}_p^e$ as:

$$\{F\}_p^e = -\int [N]^T \{p\} d(Vol) \tag{3.9}$$

the integration being carried out over the volume of the element.

In vibration problems, the external forces are replaced by the inertia forces. The nodal equivalent forces due to the inertia loading are of the form:

$$\{F_I\}_p^e = [m]^e \{\ddot{\delta}\}^e$$

where $[m]^e$ is the mass-matrix for the element. The mass matrix for the complete structure $[M]^s$ can be generated the same way as the stiffness

matrix. For the case of free vibrations, with no damping, the equation of motion becomes:

$$[K]^S\{U\} + [M]^S\{\ddot{U}\} = \{0\} \tag{3.10}$$

Assuming harmonic vibrations of frequency w,

$$\{U\} = \{U_o\} \sin wt$$

$$[K]^S\{U_o\} - w^2 [M]^S\{U_o\} = \{0\}$$

or

$$([K]^S - w^2 [M]^S)\{U_o\} = \{0\}$$

or

$$([I] - w^2 [K^{-1}]^S [M]^S)\{U_o\} = \{0\}$$

where [I] is an indentity matrix. Thus,

$$w^2 [K^{-1}]^S [M]^S \{U_o\} = \{U_o\} \tag{3.10a}$$

Equation (3.10a) indicates that if λ is an eigenvalue of $([K^{-1}]^S [M]^S)$ matrix,

$$\lambda = \frac{1}{w^2} \quad \text{or} \quad w = \frac{1}{\sqrt{\lambda}}$$

The corresponding eigenvector gives the mode shape.

The highest eigenvalue, therefore, gives the first natural frequency. The problem of determination of the natural frequencies is reduced to one of finding the eigenvalues of the $([K^{-1}]^S [M]^S)$ matrix of the structure. Since only the first few natural frequencies are of interest, the Power method can be used to find the eigen-values.

3.2 Idealization of the Fan Blade

As mentioned earlier, a fan blade may be idealized as an assembly of flat elements or curved elements. At zero speed, the fan blade is a segment of a cylindrical shell. With increased speed the blade deforms

so that the cylindrical curved elements do not remain cylindrical. If other curved elements are used the change of curvature of the elements with increasing speed would have to be considered. On the other hand, the formulation for flat plate elements is simpler since all the shapes that the fan blade may take at different speeds can be idealized by assembly of flat triangular elements. Displacement functions giving good bending stiffness for flat triangular elements are also available.

The present study has been done by idealizing the blade as an assembly of flat triangular elements as shown in Figure 3.1. The nodal points of the elements lie on the mid surface of the shell. The elements have constant thickness equal to the thickness of the blade. Five degrees of freedom per node are considered - two for in-plane deformation and three for bending. (One additional degree of freedom per node is introduced in the analysis, as explained later).

3.3. Boundary Conditions

The fan blade is rivetted along one edge, to the radial post. The post also has a "lip" under the blade (Fig. 1.5). The blade rolls on this lip as it deflects, becoming stiffer with increasing deflection.

The effect of the "lip" can be better understood by considering a cantilever, with a point load on the free-end, which comes in contact with a rigid cylindrical surface as it deflects (Fig. 3.2). This is discussed in detail by Timoshenko [41]. As the beam deflects it comes partly in contact with the rigid surface where a reaction normal to the surface is developed. With increased load, the curvature of the part of the beam in contact with the surface remains constant (equal to the

curvature of the surface), and the beam becomes stiffer because of the reduced free length. The relationship between the load and deflection under it is no longer linear.

The analysis of deflection for a plate with a similar boundary condition is very difficult especially if the plate has a distributed load.

If the vibration of the system is to be analyzed, such a boundary condition implies that harmonic oscillations of the beam or the plate cannot be assumed, and the analysis becomes extremely difficult.

However, the boundary condition may be approximated in the following two ways:

a) considering the blade built-in along one edge, without the lip. This may be referred to as "fixed boundary condition",

b) considering the blade built-in along one edge, with the lip as a flat rigid surface. The portion of the blade coming in contact with lip is assumed to be built-in on the lip. This may be referred to as "variable boundary condition".

The condition a) makes the blade less stiff than it actually is while b) makes it more stiff. The results from these two conditions can be expected to provide an upper and lower bound on the deflection and vibration characteristics of the blade. The present study has been done only for the "fixed boundary condition"(a) and can be extended for the "variable boundary condition".

3.4 Procedure for Solution

The deflection of the fan blade over the speed range of operation (0 to 5000 rpm) is large. In the present analysis only the centrifugal loading on the blade has been considered and an iterative procedure has been adopted to calculate the deflection at various speeds. Small speed increments are given in each iteration and the deflections due to the increased centrifugal loads at each step are assumed to be linear. At any speed N, the blade reaction and the centrifugal load are in equilibrium. The stiffness of the blade, and the nodal forces due to the centrifugal force can be evaluated at that speed. A small speed increment δN is then given during which the stiffness of the blade is assumed to be constant. Increments in the nodal forces due to the speed increase δN are evaluated and the deflection of the blade under this load is calculated. This deflection, when added to the initial position at speed N, gives the equilibrium position at speed $N + \delta N$. The iterative process can, thus, be started at zero speed and carried through the complete range of speed of operation.

As the blade deflects, in-plane stresses also develop in the blade, making it stiffer. This is accounted for by forming a "centrifugal stiffness" matrix. For the vibration problem, the effect of the centrifugal force field is taken into account by forming a "stiffness correction" matrix. The formulation of various matrices is discussed in the following sections.

3.5 The Stiffness Matrix

As mentioned in Chapter 2, various deflection functions for bending have been suggested in the literature for the flat triangular plate element. In the present study the deflection function used by Rawtani [18] has been used. The function is partially conforming and has been found to have good convergence and accuracy.

The local co-ordinate axes for an element are designated as x', y', z' and those for the complete blade (global axes) as x, y , z. The two co-ordinate systems are shown in Fig. 3.3. Each node of the element is considered to have five degrees-of-freedom - two for in-plane displacements and three for bending (transverse displacement and slopes). Since the in-plane stretching and bending are independent the stiffness matrices for the two can be developed separately and combined later.

The In-plane Stiffness Matrix:

Let i-j-k be the triangular element as shown in Fig. 3.3 with y' axis along the side i-j and the origin at the node i. Displacements u' and v' at any point within the element, in the direction of x' and y' axes respectively, are assumed to be linear functions of the x' and y' co-ordinates of the point, and written as:

$$u' = \beta_1 + \beta_2 x' + \beta_3 y'$$

$$v' = \beta_4 + \beta_5 x' + \beta_6 y' \qquad (3.11)$$

or in the matrix form,

$$\begin{Bmatrix} u' \\ v' \end{Bmatrix} = \begin{bmatrix} 1 & x' & y' & 0 & 0 & 0 \\ 0 & 0 & 0 & 1 & x' & y' \end{bmatrix} \begin{Bmatrix} \beta_1 \\ \beta_2 \\ \beta_3 \\ \beta_4 \\ \beta_5 \\ \beta_6 \end{Bmatrix} \tag{3.11a}$$

where β_1, $\beta_2 \ldots \beta_6$ are constants.

From the theory of elasticity, strains $\varepsilon_{x'}$, $\varepsilon_{y'}$ and $\varepsilon_{x'y'}$ are given by

$$\{\varepsilon\} = \begin{Bmatrix} \varepsilon_{x'} \\ \varepsilon_{y'} \\ \varepsilon_{x'y'} \end{Bmatrix} = \begin{Bmatrix} \dfrac{\partial u'}{\partial x'} \\ \dfrac{\partial v'}{\partial y'} \\ \dfrac{\partial u'}{\partial y'} + \dfrac{\partial v'}{\partial x'} \end{Bmatrix}$$

After substitution for u' and v' from equations (3.11)

$$\{\varepsilon\} = [B_p] \{\beta\} \tag{3.12}$$

where $[B_p]$ is given by

$$[B_p] = \begin{bmatrix} 0 & 1 & 0 & 0 & 0 & 0 \\ 0 & 0 & 0 & 0 & 0 & 1 \\ 0 & 0 & 1 & 0 & 1 & 0 \end{bmatrix}$$

and

$$\{\beta\}^T = (\beta_1, \beta_2, \beta_3, \beta_4, \beta_5, \beta_6)$$

$\{\beta\}$ can be evaluated in terms of the nodal displacements since the co-ordinates x_i', y_i', x_j', y_j' and x_k', y_k' of nodes i, j and k respectively are known. Since the origin of the co-ordinate axes is at the node i,

$$x_i' = 0$$

$$y_i' = 0$$

$$x_j' = 0$$

If nodal displacements at the nodes i, j and k are denoted by u_i', v_i', u_j', v_j' and u_k', v_k' respectively, the nodal displacements can be written in the matrix form as:

$$\begin{Bmatrix} u_i' \\ v_i' \\ u_j' \\ v_j' \\ u_k' \\ v_k' \end{Bmatrix} = [C_p] \begin{Bmatrix} \beta_1 \\ \beta_2 \\ \beta_3 \\ \beta_4 \\ \beta_5 \\ \beta_6 \end{Bmatrix}$$

or

$$\{\delta_p'\} = [C_p] \{\beta\} \tag{3.13}$$

where

$$\{\delta_p'\}^T = (u_i', \; v_i', \; u_j', \; v_j', \; u_k', \; v_k')$$

The matrix $[C_p]$ is given by

$$[C_p] = \begin{bmatrix} 1 & 0 & 0 & 0 & 0 & 0 \\ 0 & 0 & 0 & 1 & 0 & 0 \\ 1 & 0 & y_j' & 0 & 0 & 0 \\ 0 & 0 & 0 & 1 & 0 & y_j' \\ 1 & x_k' & y_k' & 0 & 0 & 0 \\ 0 & 0 & 0 & 1 & x_k' & y_k' \end{bmatrix}$$

Substituting for $\{\beta\}$ from eq. (3.13) in eq. (3.12) we get

$$\{\varepsilon\} = [B_p]\,[C_p^{-1}]\,\{\delta_p'\} \tag{3.14}$$

Assuming linear elastic behaviour of the material of the element, the stress and the strain vectors are related as follows:

$$\{\sigma\} = [D]\ \{\varepsilon\} \tag{3.15}$$

where the matrix $[D]$ is given by

$$\frac{E}{1-\mu^2}\begin{bmatrix} 1 & \mu & 0 \\ \mu & 1 & 0 \\ 0 & 0 & \frac{1-\mu}{2} \end{bmatrix}$$

μ being the Poisson's ratio and E the elastic modulus of the material.

Substituting for $\{\varepsilon\}$ from eq. (3.14) in eq. (3.15) we get,

$$\{\sigma\} = [D]\,[B_p]\,[C_p^{-1}]\,\{\delta_p'\} \tag{3.15a}$$

Using equations (3.2), (3.3) and (3.4) the stiffness matrix of the element is given by:

$$[K_p']^e = \int ([B_p][C_p^{-1}])^T [D]\ ([B_p][C_p^{-1}])\ d(Vol) \tag{3.15b}$$

Since, from matrix algebra

$$([B_p][C_p^{-1}])^T = [C_p^{-1}]^T\,[B_p]^T$$

Equation (3.15b) may, therefore, be written as:

$$[K_p']^e = [C_p^{-1}]^T\ (\int [B_p]^T[D][B_p]\ d(Vol))\ [C_p^{-1}] \tag{3.16}$$

$[C_p^{-1}]$ is a matrix of constant elements and can be taken outside the integral.

The in-plane stiffness matrix $[K_p]^e$ is a 6 x 6 symmetric matrix with non-zero positive elements on the diagonal.

The Bending Stiffness Matrix:

For the bending stiffness each node of the element is considered to have three degrees of freedom: w', the transverse displacement; $\theta_{x'}$, the rotation about the x'-axis $(\frac{\partial w'}{\partial y'})$; and $\theta_{y'}$, the rotation about the y'-axis $(-\frac{\partial w'}{\partial x'})$. The displacement function chosen is written as:

$$w' = \alpha_1+\alpha_2x'+\alpha_3y'+\alpha_4x'^2+\alpha_5x'y'+\alpha_6y'^2+\alpha_7x'^3+\alpha_8x'^2y'+\alpha_9y'^3 \tag{3.17}$$

where α_1, α_2.... α_9 are constants.

The slopes along the x' and y' axes are given by the corresponding partial derivatives as:

$$\begin{aligned}\frac{\partial w'}{\partial x'} &= \alpha_2+2\alpha_4x'+\alpha_5y'+3\alpha_7x'^2+2\alpha_8x'y' \\ \frac{\partial w'}{\partial y'} &= \alpha_3+\alpha_5x'+2\alpha_6y'+\alpha_8x'^2+3\alpha_9y'^2\end{aligned} \tag{3.17a}$$

Along the y'-axis, $x' = 0$ so that:

$$\frac{\partial w'}{\partial x'} = \alpha_2 + \alpha_5y' \tag{3.18}$$

whereas along any other line given by the equation $y' = m\,x' + C$ (edge 'i k' or 'j k' of the element), the slope is given by

$$\frac{\partial w'}{\partial x'} = \eta_1 + \eta_2\,x' + \eta_3\,x'^2 \tag{3.19}$$

where η_1, η_2 and η_3 are constants.

The two constants α_2 and α_5 in eq. (3.18) can be evaluated if $\frac{\partial w'}{\partial x'}$ at the nodes i and j is known. The slope $\frac{\partial w'}{\partial x'}$ is therefore uniquely determined along the edge 'i j' (i.e. along the y'-axis). The same is not

true for the slope $\frac{\partial w'}{\partial x'}$ along any arbitrary line since eq. (3.19) has three constants, (η_1, η_2 and η_3) which cannot be determined only from the value of $\frac{\partial w}{\partial x}$ at two points on the line. However, if two adjacent elements have y'-axis along the common edge, as shown in Fig. 3.4, the slope $\frac{\partial w'}{\partial x'}$ for the two elements along the common edge becomes compatible. Such a co-ordinate system is adopted for the elements to make the displacement function partially conforming.

The transverse displacement w' defined by equation (3.17) may be written in a matrix form as:

$$w' = [C]\{\alpha\} \tag{3.20}$$

where

$$[C] = [1,\ x',\ y',\ x'^2,\ x'y',\ y'^2,\ x'^3,\ x'^2y',\ y'^3]$$

and

$$\{\alpha\}^T = \{\alpha_1,\ \alpha_2,\ \alpha_3,\ \alpha_4,\ \alpha_5,\ \alpha_6,\ \alpha_7,\ \alpha_8,\ \alpha_9\}$$

From Equation (3.17):

$$\begin{aligned} \theta_{x'} &= \frac{\partial w'}{\partial y'} = \alpha_3+\alpha_5x'+2\alpha_6y'+\alpha_8x'^2+3\alpha_9y'^2 \\ \theta_{y'} &= -\frac{\partial w'}{\partial x'} = -\alpha_2-2\alpha_4x'-\alpha_5y'-3\alpha_7x'^2-2\alpha_8x'y' \end{aligned} \tag{3.21}$$

The nine nodal displacements and the corresponding nodal forces, expressed as vectors, are:

$$\{\delta_b'\} = [w_i',\ \theta_{x'i},\ \theta_{y'i},\ w_j',\ \theta_{x'j},\ \theta_{y'j},\ w_k',\ \theta_{x'k},\ \theta_{y'k}]^T$$

$$\{F_b'\} = [F_{z'i},\ M_{x'i},\ M_{y'i},\ F_{z'j},\ M_{x'j},\ M_{y'j},\ F_{z'k},\ M_{x'k},\ M_{y'k}]^T$$

Using equations (3.20) and (3.21), $\{\delta_b'\}$ may be written as;

$$\{\delta_b'\} = [C_b]\{\alpha\} \tag{3.22}$$

where $[C_b]$ is given by:

$$\left[\begin{array}{c|c|c|c|c|c|c|c|c}
1 & 0 & 0 & 0 & 0 & 0 & 0 & 0 & 0 \\ \hline
0 & 0 & 1 & 0 & 0 & 0 & 0 & 0 & 0 \\ \hline
0 & -1 & 0 & 0 & 0 & 0 & 0 & 0 & 0 \\ \hline
1 & 0 & y_j' & 0 & 0 & y_j'^2 & 0 & 0 & y_j'^3 \\ \hline
0 & 0 & 1 & 0 & 0 & 2y_j' & 0 & 0 & 3y_j'^2 \\ \hline
0 & -1 & 0 & 0 & -y_j' & 0 & 0 & 0 & 0 \\ \hline
1 & x_k' & y_k' & x_k'^2 & x_k' y_k' & y_k'^2 & x_k'^3 & x_k'^2 y_k' & y_k'^3 \\ \hline
0 & 0 & 1 & 0 & x_k' & 2y_k' & 0 & x_k'^2 & 3y_k'^2 \\ \hline
0 & -1 & 0 & -2x_k' & -y_k' & 0 & -3x_k'^2 & -2x_k' y_k' & 0
\end{array}\right]$$

Therefore, $\{\alpha\} = [C_b^{-1}]\ \{\delta_b'\}$ (3.22a)

From the flat-plate theory, the strain vector is given by:

$$\{\varepsilon\} = \begin{Bmatrix} \varepsilon_{x'x'} \\ \varepsilon_{y'y'} \\ \varepsilon_{x'y'} \end{Bmatrix} = \begin{Bmatrix} -z' \dfrac{\partial^2 w'}{\partial x'^2} \\ -z' \dfrac{\partial^2 w'}{\partial y'^2} \\ -2z' \dfrac{\partial^2 w'}{\partial x' \partial y'} \end{Bmatrix} \qquad (3.23)$$

From eq. (3.17) and eq. (3.21) we get:

$$\frac{\partial^2 w'}{\partial x'^2} = 2\alpha_4 + 6\alpha_7 x' + 2\alpha_8 y'$$

$$\frac{\partial^2 w'}{\partial y'^2} = 2\alpha_6 + 6\alpha_9 y'$$

$$2\frac{\partial^2 w'}{\partial x' \partial y'} = 2\alpha_5 + 4\alpha_8 x'$$

The strain vector from eq. (3.23) may be written as:

$$\{\varepsilon\} = -z'[B_b]\{\alpha\} \tag{3.24}$$

where $[B_b]$ is given by

$$\begin{bmatrix} 0 & 0 & 0 & 2 & 0 & 0 & 6x' & 2y' & 0 \\ 0 & 0 & 0 & 0 & 0 & 2 & 0 & 0 & 6y' \\ 0 & 0 & 0 & 0 & 2 & 0 & 0 & 4x' & 0 \end{bmatrix}$$

Substituting for $\{\alpha\}$ from eq. (3.22a) in eq. (3.24) we get

$$\{\varepsilon\} = -z'[B_b][C_b^{-1}]\{\delta_b'\} \tag{3.25}$$

The relation between the stress vector$\{\sigma\}$ and the strain vector $\{\varepsilon\}$ is given by

$$\{\sigma\} = [D]\{\varepsilon\} \tag{3.26}$$

where $[D]$ is defined by eq. (3.15).

As in the case of the in-plane stiffness matrix, the bending stiffness matrix is now given by:

$$[K_b']^e = [C_b^{-1}]^T \left(\int_{Vol} [B_b]^T[D][B_b]\, (z'^2)\, d(Vol)\right)[C_b^{-1}] \tag{3.27}$$

The volume integral can be reduced to an area integral by integrating out z'^2. Since z' does not appear in any of the matrices we may write eq. (3.27) in the form

$$[K_b']^e = [C_b^{-1}]^T \left(\int_{Vol} z'^2\, [f(x', y')]\, d(Vol)\right)[C_b^{-1}]$$

where $[f(x', y')]$ represents the matrix product in the integral in eq. (3.27). Therefore,

$$[K_b']^e = [C_b^{-1}]^T \left(\int_{x'}\int_{y'}\int_{z'} z'^2\, [f(x', y')]\, dx'\, dy'\, dz'\right)[C_b^{-1}]$$

or

$$[K_b']^e = [C_b^{-1}]^T \left(\int_{x'} \int_{y'} \frac{t^3}{12} [f(x',y')] dx' \, dy' \right) [C_b^{-1}]$$

since

$$\int_{-t/2}^{+t/2} z'^2 \, dz' = \frac{t^3}{12}$$

where t is the thickness of the element.

For computational purposes the factor $\frac{t^3}{12}$ can be combined with the factor $\frac{E}{(1-\mu^2)}$ of matrix $[D]$ in eq. (3.27). Therefore, for bending stiffness calculation $[D]$ is given by:

$$[D] = \begin{bmatrix} 1 & \mu & 0 \\ \mu & 1 & 0 \\ 0 & 0 & \frac{1-\mu}{2} \end{bmatrix}$$

and the final expression for the element bending stiffness can be written as:

$$[K_b']^e = \frac{Et^3}{12(1-\mu^2)} [C_b^{-1}]^T \left(\int_{x'} \int_{y'} [B_b]^T [D] [B_b] dx' \, dy' \right) [C_b^{-1}]$$

or

$$[K_b']^e = \frac{Et^3}{12(1-\mu^2)} [C_b^{-1}]^T \left(\int_{x} \int_{y} [BB] dx' dy' \right) [C_b^{-1}] \qquad (3.28)$$

where

$$[BB] = [B_b]^T [D] [B_b]$$

and is written as shown on the next page.

$$
\begin{bmatrix}
0 & & & & & & & & \\
0 & 0 & & & & & & & \\
0 & 0 & 0 & & & & & & \\
0 & 0 & 0 & 4 & \multicolumn{5}{c}{\text{Symmetric}} \\
0 & 0 & 0 & 0 & 2(1-\mu) & & & & \\
0 & 0 & 0 & 4\mu & 0 & 4 & & & \\
0 & 0 & 0 & 12x' & 0 & 12\mu x' & 36x'^2 & & \\
0 & 0 & 0 & 4y' & 4(1-\mu)x' & 4\mu y' & 12x'y' & 4y'^2+8(1-\mu)x'^2 & \\
0 & 0 & 0 & 12\mu y' & 0 & 12y' & 36\mu x'y' & 12\mu y'^2 & 36y'^2
\end{bmatrix}
$$

$[K_b']^e$ obtained from eq. (3.28) is a 9 x 9 symmetric matrix with non-zero positive diagonal elements. The total stiffness matrix of the element is obtained by combining the in-plane and the bending stiffness matrices. The in-plane stiffness matrix is composed of 2 x 2 sub-matrices as shown below:

$$
[K_p']^e = \left[\begin{array}{c|c|c}
K_p'^{11} & K_p'^{12} & K_p'^{13} \\
\hline
K_p'^{21} & K_p'^{22} & K_p'^{23} \\
\hline
K_p'^{31} & K_p'^{32} & K_p'^{33}
\end{array}\right]
$$

and the bending stiffness matrix is composed of 3 x 3 sub-matrices as:

$$[K_b']^e = \begin{bmatrix} K_b'^{11} & K_b'^{12} & K_b'^{13} \\ K_b'^{21} & K_b'^{22} & K_b'^{23} \\ K_b'^{31} & K_b'^{32} & K_b'^{33} \end{bmatrix}$$

Before combining these stiffness matrices it may be noted that displacements prescribed for the "in-plane" forces do not affect the bending deformations and vice versa. Also, the rotation $\theta_{z'}$ does not enter as a parameter into the definitions of the deformation in either mode. However for reasons of transformation and assembly, discussed in the next section, this displacement is taken into account by associating with it a fictitious couple $M_{z'}$ and inserting appropriate number of zeros in the stiffness matrix corresponding to rows and columns of $\theta_{z'}$.

The total displacement vector for each node now is

$$\{\delta_i'\}^e = \begin{Bmatrix} u_i' \\ v_i' \\ w_i' \\ \theta_{x'i} \\ \theta_{y'i} \\ \theta_{z'i} \end{Bmatrix}$$

and the corresponding force vector is:

$$\{F'_i\}^e = \begin{Bmatrix} F_{x'i} \\ F_{y'i} \\ F_{z'i} \\ M_{x'i} \\ M_{y'i} \\ M_{z'i} \end{Bmatrix}$$

The total stiffness matrix, therefore, is of size 18 x 18 and is composed of 6 x 6 sub-matrices as follows

$$[K']^e = \begin{bmatrix} K'^{11} & K'^{12} & K'^{13} \\ K'^{21} & K'^{22} & K'^{23} \\ K'^{31} & K'^{32} & K'^{33} \end{bmatrix} \qquad (3.29)$$

where each sub-matrix is given by

$$[K']^{\gamma S} = \begin{bmatrix} K_p'^{\gamma S} & \begin{matrix} 0 & 0 & 0 \\ 0 & 0 & 0 \end{matrix} & \begin{matrix} 0 \\ 0 \end{matrix} \\ \begin{matrix} 0 & 0 \\ 0 & 0 \\ 0 & 0 \end{matrix} & K_b'^{\gamma S} & \begin{matrix} 0 \\ 0 \\ 0 \end{matrix} \\ \begin{matrix} 0 & 0 \end{matrix} & \begin{matrix} 0 & 0 & 0 \end{matrix} & 0 \end{bmatrix}$$

The element stiffness matrix now has to be transformed to the global co-ordinate system.

3.6 Transformation to Global Co-ordinates

The global co-ordinate system has the co-ordinate axes x, y and z. The displacements and the nodal forces in the local and the global co-ordinate systems are related by the transformation:

$$\{\delta_i'\} = [L]\{\delta_i\}$$

and

$$\{F_i'\} = [L]\{F_i\}$$

where

$$[L] = \begin{bmatrix} \lambda & 0 \\ 0 & \lambda \end{bmatrix} \tag{3.30}$$

with $[\lambda]$ being the 3 x 3 matrix of the direction cosines of the angles formed between the local and the global axes; i.e.

$$[\lambda] = \begin{bmatrix} \ell_x & m_x & n_x \\ \ell_y & m_y & n_y \\ \ell_z & m_z & n_z \end{bmatrix} \tag{3.30a}$$

where (ℓ_x, m_x, n_x); (ℓ_y, m_y, n_y); (ℓ_z, m_z, n_z) are the direction cosines of x', y', z' axes, respectively, with the global x, y, z axes.

The matrix [L] is a 6 x 6 matrix and relates the six co-ordinates in the local system - namely x', y', z' and the rotations $\theta_{x'}$, $\theta_{y'}$, $\theta_{z'}$ about these axes respectively - to the corresponding co-ordinates in the global system. However, in defining the degrees-of-freedom for each node of an element only two rotations - $\theta_{x'}$ and $\theta_{y'}$ - have been considered. A dummy rotation, $\theta_{z'}$, and a corresponding fictitious couple, is needed in order to use the transformation matrix

[L]. This is achieved by introducing zeros in the 6th, 12th and 18th, rows and columns of the stiffness matrix of an element, as indicated in Section 3.5.

When the local and global co-ordinates are cartesian, the matrix [L] is orthogonal. Therefore, using eq. (3.5), the stiffness matrix of the element in the global co-ordinates becomes:

$$[K]^e = [T]^T [K']^e [T]$$

in which

$$[T] = \begin{bmatrix} L & 0 & 0 \\ 0 & L & 0 \\ 0 & 0 & L \end{bmatrix} \qquad (3.30b)$$

The direction cosines can be evaluated from the following set of equations:

$$A = y'_{ji}\, z'_{Ki} - y'_{Ki}\, z'_{ji}$$

$$B = x'_{Ki}\, z'_{ji} - x'_{ji}\, z'_{Ki}$$

$$C = x'_{ji}\, y'_{Ki} - x'_{Ki}\, y'_{ji}$$

$$F = \sqrt{x'^2_{ji} + y'^2_{ji} + z'^2_{ji}}$$

$$G = -\sqrt{A^2 + B^2 + C^2}$$

$$\ell_z = A/G, \quad m_z = B/G, \quad n_z = C/G$$

$$\ell_y = x'_{ji}/F, \quad m_y = y'_{ji}/F, \quad n_y = z'_{ji}/F$$

$$\ell_x = m_y n_z - m_z n_y$$

$$m_x = \ell_z n_y - n_z \ell_y$$

$$n_x = \ell_y m_z - m_y \ell_z$$

where

$$y'_{ji} = y'_j - y'_i \quad \text{etc.}$$

The method of assembling the element stiffness matrix into the system stiffness matrix is indicated in Fig. (3.5). It may be noted that the 18 x 18 stiffness matrix of the element, in the global co-ordinates, is singular. The reason for this is the insertion of zeros in the rows and columns corresponding to the $\theta_{z'}$ displacement in the stiffness matrix in the local co-ordinates. After transformation, therefore, there is a constant ratio between the adjacent rows and columns 5 and 6, 11 and 12, and 17 and 18. However, since an element inside the structure shares the nodes with other elements not in the same plane, this singularity disappears when the elements of the stiffness matrices of all these elements are suitably added in assembly of system stiffness.

Difficulty arises for the nodes at the edge of the blade where all the elements joining at a particular node are in the same plane (nodes 3, 6 and 9 in Fig. 3.5). Transformation for these nodes is done such that the lateral displacements (u', v' and w') are transferred to the global co-ordinates while the angular rotations ($\theta_{x'}$, $\theta_{y'}$ and $\theta_{z'}$) are transferred to a new co-ordinate system, x'', y'', z'', in the plane of the edge nodes. This co-ordinate system is indicated in Fig. (3.6). The transformation matrix for the edge nodes is, therefore, given by:

$$[L] = \begin{bmatrix} \lambda & 0 \\ 0 & \lambda'' \end{bmatrix}$$

where $[\lambda'']$ is a 3 x 3 sub-matrix of direction cosines of the angles formed between the local axes and the x'', y'', z'' axes.

For the reasons mentioned above, the singularity in the matrix is removed by deleting, after transformation, the rows and columns numbered 6, 12 and 18 in the element stiffness matrix.

For the complete system, therefore, all the nodes have six degrees of freedom each except the nodes on the edge (where all elements meeting are in the same plane), which have five degrees of freedom each.

3.7 Centrifugal Stiffness Matrix

In the absence of the in-plane stresses in the element, the stiffness matrix is given by eq. (3.29). However, in the presence of the in-plane stresses, the strain energy stored due to bending is higher since the transverse deflection introduces in-plane strains.

If the in-plane stresses are given by $\sigma_{x'}$, $\sigma_{y'}$ and $\tau_{x'y'}$, the strain energy stored in the element is higher than the usual bending strain energy by the amount

$$U_1 = \frac{1}{2}\int\left[\sigma_{x'}\left(\frac{\partial w'}{\partial x'}\right)^2 + \sigma_{y'}\left(\frac{\partial w'}{\partial y'}\right)^2 + 2\tau_{x'y'}\left(\frac{\partial w'}{\partial y'}\right)\left(\frac{\partial w'}{\partial x'}\right)\right] d\,(\text{Vol}) \tag{3.31}$$

Equation (3.31) may be written as:

$$U_1 = \frac{1}{2}\iint t \begin{Bmatrix} \frac{\partial w'}{\partial x'} \\ \frac{\partial w'}{\partial y'} \end{Bmatrix}^T \begin{bmatrix} \sigma_{x'} & \tau_{x'y'} \\ \tau_{x'y} & \sigma_{y'} \end{bmatrix} \begin{Bmatrix} \frac{\partial w'}{\partial x'} \\ \frac{\partial w'}{\partial y'} \end{Bmatrix} dx'\, dy' \tag{3.32}$$

This energy leads to an increase in the bending stiffness matrix of the element by the amount

$$[K'_{cs}] = \iint t[G]^T \begin{bmatrix} \sigma_{x'} & \tau_{x'y} \\ \tau_{x'y} & \sigma_{y'} \end{bmatrix} [G]\, dx'\, dy' \tag{3.33}$$

where [G] is defined by the relation

$$\begin{Bmatrix} \frac{\partial w'}{\partial x'} \\ \frac{\partial w'}{\partial y'} \end{Bmatrix} = [G]\,\{\delta'_b\} \tag{3.33a}$$

The proof of equation (3.33) is given by Kapur and Hartz [42] while dealing with the problem of stability of plates.

From equation (3.17a)

$$\begin{Bmatrix} \frac{\partial w'}{\partial x'} \\ \frac{\partial w'}{\partial y'} \end{Bmatrix} = [H] \begin{Bmatrix} \alpha_1 \\ \alpha_2 \\ \vdots \\ \alpha_9 \end{Bmatrix} \tag{3.33b}$$

where $[H]$ is given by

$$\begin{bmatrix} 0 & 1 & 0 & 2x' & y' & 0 & 3x'^2 & 2x'y' & 0 \\ 0 & 0 & 1 & 0 & x' & 2y' & 0 & x'^2 & 3y'^2 \end{bmatrix}$$

Substituting for $\{\alpha\}$ from eq. (3.22a) in eq. (3.33b) we get

$$\begin{Bmatrix} \frac{\partial w'}{\partial x'} \\ \frac{\partial w'}{\partial y'} \end{Bmatrix} = [H] [C_b^{-1}] \{\delta_b^e\} \tag{3.33c}$$

Substituting eq. (3.33c) in eq. (3.33) we get

$$[K'_{cs}] = t [C_b^{-1}]^T \left(\iint [H]^T \begin{bmatrix} \sigma_{x'} & \tau_{x'y'} \\ \tau_{x'y} & \sigma_{y'} \end{bmatrix} [H] \, dx' \, dy' \right) [C_b^{-1}] \tag{3.34}$$

$[K'_{cs}]$ is a 9 x 9 matrix. This is to be added to the bending stiffness matrix of the element to get total bending stiffness matrix, before combining with the in-plane stiffness matrix to get the total stiffness matrix of the element.

Equation (3.34) may be written as

$$[K'_{cs}] = t [C_b^{-1}]^T \left(\iint [Z] \, dx' \, dy' \right) [C_b^{-1}]$$

where

$$[Z] = [H]^T \begin{bmatrix} \sigma_{x'} & \tau_{x'y'} \\ \tau_{x'y'} & \sigma_{y'} \end{bmatrix} [H]$$

[Z] is a symmetric 9 x 9 matrix. The elements of this matrix are defined in Appendix I.

The stresses $\sigma_{x'}$, $\sigma_{y'}$, $\tau_{x'y'}$ can be evaluated if the deflected position of the element is known. Using the subscripts 'n' and 'o' for the new and the original co-ordinates respectively, the vector of nodal in-plane displacements may be written as

$$\begin{Bmatrix} u_i' \\ v_i' \\ u_j' \\ v_j' \\ u_k' \\ v_k' \end{Bmatrix} = \begin{Bmatrix} o \\ o \\ o \\ y'_{jn} - y'_{jo} \\ x'_{kn} - x'_{ko} \\ y'_{kn} - y'_{ko} \end{Bmatrix} = \{\delta_p'\}$$

The stress vector is then given by eq. (3.15a).

3.8 Centrifugal Loading

The centrifugal force at any point on the mid surface of the blade can be evaluated from the principles of dynamics. Consider a point (x, y, z) on the mid surface of the rotating blade when the blade is vibrating. If the instantaneous position of point is (x + u), (y + v) and (z + w), with velocity components $\dot{u}$, $\dot{v}$ and $\dot{w}$ and acceleration $\ddot{u}$, $\ddot{v}$ and $\ddot{w}$, the components of the centrifugal force in the directions of the x, y z axes are given by

$$F_x = \rho(x + u)\Omega^2 - 2\rho\Omega\dot{w}\cos\theta - 2\rho\Omega\dot{v}\sin\theta - \rho\ddot{u}$$

$$F_y = \rho(y + v)\Omega^2 \sin^2\theta + \rho(z + w)\Omega^2 \sin\theta\cos\theta + 2\rho\Omega\dot{u}\sin\theta - \rho\ddot{v} \quad (3.35)$$

$$F_z = \rho(z + w)\Omega^2 \cos^2\theta + \rho(y + v)\Omega^2 \sin\theta\cos\theta + 2\rho\Omega\dot{u}\cos\theta - \rho\ddot{w}$$

where

ρ = density of the material of the blade

Ω = speed of rotation of the fan

θ = angle made by the blade post with the axis of rotation.

The details of the evaluation of D'Alembert forces at any point on the blade are presented in Appendix II. When the blade is not vibrating, the displacement (u, v, w) of any point is zero. Eqs. (3.35) for a rotating non-vibrating blade reduce to:

$$F_x = \rho x\,\Omega^2$$

$$F_y = \rho y\,\Omega^2 \sin^2\theta + \rho z\Omega^2 \sin\theta\cos\theta \quad (3.36)$$

$$F_z = \rho z\,\Omega^2 \cos^2\theta + \rho y\Omega^2 \sin\theta\cos\theta$$

To calculate the deflection of the blade, the centrifugal force given by eq. (3.36) is used as the external load on the blade. Eq. (3.36) gives the forces in the direction of the global co-ordinate axes.

The D'Alembert forces in eq. (3.36) are expressed in terms of the global co-ordinates x, y, z of a point. For the convenience of computation it is better to express F_x, F_y, F_z in terms of the local

co-ordinates of the point. The global and the local co-ordinates of a point are related by the expression

$$\begin{Bmatrix} x \\ y \\ z \end{Bmatrix} = \begin{bmatrix} \ell_x & \ell_y & \ell_z \\ m_x & m_y & m_z \\ n_x & n_y & n_z \end{bmatrix} \begin{Bmatrix} x' \\ y' \\ z' \end{Bmatrix} + \begin{Bmatrix} x_i \\ y_i \\ z_i \end{Bmatrix} \qquad (3.36a)$$

where x', y', z' are the local co-ordinates of the point ($z' = 0$) and x_i, y_i, z_i are the global co-ordinates of the node i of the triangular element in which the point is located.

From equation (3.36a)

$$x = (x'\ell_x + y'\ell_y) + x_i$$

$$y = (x'm_x + y'm_y) + y_i$$

$$z = (x'n_x + y'n_y) + z_i$$

Substituting these in eq. (3.36), the expressions for F_x, F_y and F_z can be written as

$$F_x = \Omega^2\rho\{x'\ell_x + y'\ell_y + x_i\}$$

$$F_y = \Omega^2\rho\{x'(m_x \sin^2\theta + n_x \sin\theta\cos\theta) + y'(m_y \sin^2\theta + n_y \sin\theta\cos\theta) + y_i \sin^2\theta + z_i \sin\theta\cos\theta\} \qquad (3.36b)$$

$$F_z = \Omega^2\rho\{x'(m_x \sin\theta\cos\theta + n_x \cos^2\theta) + y'(m_y \sin\theta\cos\theta + n_y \cos^2\theta) + y_i \sin\theta\cos\theta + z_i \cos^2\theta\}$$

3.9 Nodal Equivalent of the Distributed Centrifugal Force

The centrifugal force, per unit volume, given by eqs. (3.36) or (3.36b) can be transformed to local co-ordinates by the relation

$$\begin{Bmatrix} F_{x'} \\ F_{y'} \\ F_{z'} \end{Bmatrix} = [L] \begin{Bmatrix} F_x \\ F_y \\ F_z \end{Bmatrix}$$

[L] being the matrix of direction cosines as in eq. (3.30a).

The nodal equivalent forces are found by the principle of virtual work. The nodal displacements on which which these forces do work are given by the vector

$$\begin{Bmatrix} u' \\ v' \\ w' \end{Bmatrix}$$

From eqs. (3.11) and (3.17)

$$\begin{Bmatrix} u' \\ v' \\ w' \end{Bmatrix} = [N] \begin{Bmatrix} \beta_1 \\ \beta_2 \\ \vdots \\ \beta_6 \\ \\ \alpha_1 \\ \vdots \\ \alpha_9 \end{Bmatrix} \tag{3.38}$$

where [N] is given by

$$\left[\begin{array}{cccccc|c} 1 & x' & y' & 0 & 0 & 0 & \\ 0 & 0 & 0 & 1 & x' & y' & 0 \\ \hline & & 0 & & & & 1 \; x' \; y' \; x'^2 \; x'y' \; y'^2 \; x'^3 \; x'^2y' \; x'y'^2 \; y'^3 \end{array}\right]$$

From equation (3.11a)

$$\begin{Bmatrix} u' \\ v' \end{Bmatrix} = [N_p]\,\{\beta\} \tag{3.38a}$$

where $[N_p]$ is given by

$$\begin{bmatrix} 1 & x' & y' & 0 & 0 & 0 \\ 0 & 0 & 0 & 1 & x' & y' \end{bmatrix}$$

Substituting for $\{\beta\}$ from eq. (3.13) in eq. (3.38a) we get

$$\begin{Bmatrix} u' \\ v' \end{Bmatrix} = [N_p]\,[C_p^{-1}]\,\{\delta_p'\} \tag{3.39}$$

Similarly, substituting for $\{\alpha\}$ from eq. (3.22a) in eq. (3.20), we get

$$\{w'\} = [C]\,[C_b^{-1}]\,\{\delta_b'\} \tag{3.40}$$

Combining eq. (3.39) and eq. (3.40) leads to

$$\begin{Bmatrix} u' \\ v' \\ w' \end{Bmatrix} = [N]\,[P^{-1}]\,\{\delta_{15}'\} \tag{3.41}$$

where $\{\delta_{15}'\}$ is a vector of the in-plane and bending displacements (this vector has 15 elements), $[N]$ is given by eq. (3.38), and $[P]$ is defined by the following equation:

$$\{\delta_{15}'\} = [P] \begin{Bmatrix} \beta_1 \\ \vdots \\ \beta_6 \\ \alpha_1 \\ \vdots \\ \alpha_9 \end{Bmatrix} \tag{3.42}$$

Eq. (3.42) can also be written as

$$\begin{Bmatrix} u_i' \\ v_i' \\ w_i' \\ \theta_{x'i} \\ \theta_{y'i} \\ u_j' \\ \vdots \\ \theta z'_i \end{Bmatrix} = \begin{bmatrix} \begin{bmatrix} N_p & 0 \\ 0 & N_b \end{bmatrix}_{\substack{x'=0 \\ y'=0}} \\ \begin{bmatrix} N_p & 0 \\ 0 & N_b \end{bmatrix}_{\substack{x'=0 \\ y'=y_j'}} \\ \begin{bmatrix} N_p & 0 \\ 0 & N_b \end{bmatrix}_{\substack{x'=x_K' \\ y'=y_K'}} \end{bmatrix}$$

where

$$\begin{bmatrix} N_p & 0 \\ 0 & N_b \end{bmatrix} = \left[\begin{array}{cccccc|c} 1 & x & y & 0 & 0 & 0 & \\ 0 & 0 & 0 & 1 & x & y & 0 \\ \hline & & & & & & 1 \; x' \; y' \; x'^2 \; x'y' \; y'^2 \; x'^3 \; x'^2y' \; x'y'^2 \; y'^3 \\ & & 0 & & & & 0 \; 0 \; 1 \; 0 \; x' \; 2y' \; 0 \; x'^2 \; 3y'^2 \\ & & & & & & 0 \; -1 \; 0 \; -2x' \; -y' \; 0 \; -3x'^2 \; -2x'y' \; 0 \end{array}\right]$$

Let a virtual arbitrary displacement $\{\delta'^{*}_{15}\}$ be given at the nodes. The virtual displacement within the element is given by:

$$\begin{Bmatrix} u^* \\ v^* \\ w^* \end{Bmatrix} = [N]\,[P^{-1}]\,\{\delta'^{*}_{15}\}$$

Equating the external and the internal work done, we get:

$$\{\delta'^{*}_{15}\}^T \{F'_{15}\} = -\{\delta'^{*}_{15}\}^T [P^{-1}]^T \left(\iint \pm [N]^T \begin{Bmatrix} F^*_{x'} \\ F^*_{y'} \\ F^*_{z'} \end{Bmatrix} dx'\, dy'\right)$$

Since the equality should hold for all arbitrary virtual displacements,

$$\{F'_{15}\} = - [P^{-1}]^T \left(\iint \pm [N]^T \begin{Bmatrix} F^*_{x'} \\ F^*_{y'} \\ F^*_{z'} \end{Bmatrix} dx'\, dy'\right) \tag{3.43}$$

Eq. (3.43) may also be written as:

$$\{F'_{15}\} = - \pm [P^{-1}]^T \left(\iint [NF]\, dx'\, dy'\right) \tag{3.43a}$$

where

$$[NF] = [N] \begin{Bmatrix} F_{x'} \\ F_{y'} \\ F_{z'} \end{Bmatrix}$$

The vector $\{F'_{15}\}$ is the vector of the nodal equivalent forces. Elements of [NF] are defined in Appendix III.

This nodal force vector is in the local co-ordinates and has to be transformed to the global co-ordinates before assembly in the vector for the complete system. Before transformation this vector is converted into a vector of 18 elements by inserting zeros in the 6th, 12th and 18th rows, as in the stiffness matrix. The transformation is carried out by the relation

$$\{F\}^e_g = [T]^T \{F'\}^e_\ell \tag{3.44}$$

where the transformation matrix [T] is given by eq. (3.30b).

The nodal force vectors for all the elements are evaluated and assembled in the force vector for the complete system, $\{F\}^S$, following the same procedure as in the case of the stiffness matrices.

3.10 Calculation of the Deflections

As explained in the preceding sections, at any position of the blade, the stiffness matrix $[K]^S$ of the blade can be computed. For a small increment in speed the increase in the nodal force vector $\{F\}^S$ can be evaluated, and the deflection vector $\{\delta\}^S$ due to this increment in loading is found by the equilibrium relation

$$[K]^S \{\delta\}^S + \{F\}^S = \{0\}$$

or

$$\{\delta\}^S = - [K^{-1}]^S \{F\}^S$$

This displacement vector, when added to the initial position of the blade, gives the new position at the increased speed.

The speed increment is assumed to be small so that the assumption of linear force-displacement relationship is valid.

3.11 The Vibration Problem

The general expression for the inertia (D'Alembert) force, per unit volume, at a point on the blade has been derived in Appendix II, and written as eq. (3.35) in the preceding section. The equations may be rewritten as:

$$\begin{aligned} F_x &= F_{x1} + F_{x2} + F_{x3} + F_{x4} \\ F_y &= F_{y1} + F_{y2} + F_{y3} + F_{y4} \\ F_z &= F_{z1} + F_{z2} + F_{z3} + F_{z4} \end{aligned} \qquad (3.45)$$

where

$$
\begin{aligned}
F_{x1} &= \rho\Omega^2 x \\
F_{y1} &= \rho\Omega^2 (y \sin^2\theta + z \sin\theta \cos\theta) \\
F_{z1} &= \rho\Omega^2 (z \cos^2\theta + y \sin\theta \cos\theta)
\end{aligned}
\tag{3.46}
$$

$$
\begin{aligned}
F_{x2} &= \rho\Omega^2 u \\
F_{y2} &= \rho\Omega^2 (v \sin^2\theta + z \sin\theta \cos\theta) \\
F_{z2} &= \rho\Omega^2 (w \cos^2\theta + v \sin\theta \cos\theta)
\end{aligned}
\tag{3.47}
$$

$$
\begin{aligned}
F_{x3} &= \rho\Omega (2 \dot{w} \cos\theta + 2 \dot{v} \sin\theta) \\
F_{y3} &= \rho\Omega (2 \dot{u} \sin\theta) \\
F_{z3} &= \rho\Omega (2 \dot{u} \cos\theta)
\end{aligned}
\tag{3.48}
$$

$$
\begin{aligned}
F_{x4} &= -\rho \ddot{u} \\
F_{y4} &= -\rho \ddot{v} \\
F_{z4} &= -\rho \ddot{w}
\end{aligned}
\tag{3.49}
$$

As mentioned earlier, when the blade is not vibrating, only the components F_{x1}, F_{y1}, F_{z1} are acting. Only these components need be considered to evaluate the equilibrium position of the blade at any speed. For the vibration analysis at any equilibrium position, the components

given by eqs. (3.47), (3.48) and (3.49) constitute the D'Alembert forces acting on a point on the blade. The nodal equivalents of these forces can be found following the procedure outlined earlier. The components F_{x2}, F_{y2}, F_{z2} give the nodal equivalent force vector $\{F\}_2$ as a relation

$$\{F\}_2 = [K_{sc}]^S \{\delta\}$$

where $\{\delta\}$ is a vector of the nodal displacements and $[K_{sc}]$ is a matrix termed "Stiffness Correction Matrix" for the structure. The components F_{x4}, F_{y4} and F_{z4} give the nodal equivalent force vector $\{F\}_4$ as a relation

$$\{F\}_4 = [M]^S \{\ddot{\delta}\}$$

where $[M]^S$ is the "Mass Matrix" for the structure. The components F_{x3}, F_{y3} and F_{z3} are due to the Coriolis acceleration. These have been neglected in the present analysis. These components, being proportional to velocity, lead to a matrix similar to a damping matrix and produce phase shift.

For free vibrations, the equation of motion for the structure can be written as

$$[K]^S \{\delta\} = [K_{sc}]^S \{\delta\} - [M]^S \{\ddot{\delta}\}$$

or

$$[K]^S \{\delta\} - [K_{sc}]^S \{\delta\} + [M]^S \{\ddot{\delta}\} = \{0\} \qquad (3.50)$$

Assuming harmonic vibrations of the form

$$\{\delta\} = \{\delta_o\} \sin wt$$

where w = natural frequency, eq. (3.50) may be written as:

$$([K]^s - [K_{sc}]^s) - w^2[M]^s)\{\delta_o\} = \{0\} \qquad (3.50a)$$

Writing $[K_c]^s = [K]^s - [K_{sc}]^s$, eq. (3.50a) reduces to

$$([K_c]^s - w^2 [M]^s)\{\delta_o\} = \{0\}$$

or

$$([I] - w^2 [K_c^{-1}]^s [M]^s)\{\delta_o\} = \{0\} \qquad (3.51)$$

where [I] is the identity matrix.

Eq. (3.51) is a standard eigenvalue problem. If λ is an eigenvalue of $[K_c^{-1}]^s [M]^s$ matrix

$$\lambda = \frac{1}{w^2} \quad \text{or} \quad w = \frac{1}{\sqrt{\lambda}}$$

The corresponding eigenvector gives the mode shape for that frequency. The fundamental frequency is thus obtained from the highest eigenvalue.

The formulation of the additional matrices for the vibration problem is discussed in the subsequent sections.

3.12 The Stiffness Correction Matrix

Equation (3.47) may be written as

$$\begin{Bmatrix} F_{x2} \\ F_{y2} \\ F_{z2} \end{Bmatrix} = \rho\Omega^2 \; [R] \begin{Bmatrix} u \\ v \\ w \end{Bmatrix} \qquad (3.52)$$

where

$$[R] = \begin{bmatrix} 1 & 0 & 0 \\ 0 & \sin^2\theta & \sin\theta\cos\theta \\ 0 & \sin\theta\cos\theta & \cos^2\theta \end{bmatrix}$$

In the local co-ordinates, eq. (3.52) becomes

$$\begin{Bmatrix} F_{x'2} \\ F_{y'2} \\ F_{z'2} \end{Bmatrix} = \rho\Omega^2 \; [Q] \begin{Bmatrix} u' \\ v' \\ w' \end{Bmatrix}$$

where $[Q] = [\lambda]\,[R]\,[\lambda]^T$

$[\lambda]$ being the matrix of direction cosines.

The nodal equivalent force vector $\{F_2'\}_{15}$ can be found following the steps in eq. (3.41) through eq. (3.43) and is given by

$$\{F_2'\}_{15} = -[PP]\,\{\delta'_{15}\}$$

where

$$[PP] = \rho t\Omega^2\,[P^{-1}]^T \left(\iint [NQ]\,dx'\,dy'\right)[P^{-1}] \qquad (3.53)$$

and

$$[NQ] = [N]^T\,[Q]\,[N]$$

$[NQ]$ is a 15 x 15 symmetric matrix and its elements are defined in Appendix IV.

Introducing the fictitious moment $M_{z'}$, the nodal force vector of 18 elements is given by

$$\{F_2'\} = -[K'_{sc}]^e\,\{\delta\} \qquad (3.53a)$$

where

$$[K'_{sc}]^e = \begin{bmatrix} K'^{11}_{sc} & K'^{12}_{sc} & K'^{13}_{sc} \\ K'^{21}_{sc} & K'^{22}_{sc} & K'^{23}_{sc} \\ K'^{31}_{sc} & K'^{32}_{sc} & K'^{33}_{sc} \end{bmatrix}$$

and

$$[K'^{\gamma s}_{sc}] = \left[\begin{array}{c|c} PP^{\gamma s} & 0 \\ \hline 0 & 0 \end{array}\right]$$

$[PP]^{\gamma s}$ being the 5 x 5 sub-matrix obtained by partitioning the 15 x 15 matrix [PP] of eq. (3.53).

The matrix $[K'_{sc}]^e$ can be transformed to the global co-ordinates and assembled into the stiffness correction matrix of the system, $[K_{sc}]^s$.

3.13 The Mass Matrix

The mass matrix results from the components F_{x4}, F_{y4}, F_{z4} of the D'Alembert forces. The mass matrices for the in-plane and the bending components can be generated separately for each element.

The in-plane Mass Matrix:

The inertia forces, per unit volume, at a point due to the in-plane accelerations may be written as:

$$\begin{Bmatrix} F_{x'4} \\ F_{y'4} \end{Bmatrix} = -\rho \begin{Bmatrix} \ddot{u}' \\ \ddot{v}' \end{Bmatrix}$$

Using eqs. (3.11), (3.12) and (3.13) we get

$$\begin{Bmatrix} F_{x'4} \\ F_{y'4} \end{Bmatrix} = -\rho\,[N_p]\,[C_p^{-1}]\,\{\ddot{\delta}_p'\} \tag{3.54}$$

The nodal equivalent forces for the element are then given by

$$\begin{Bmatrix} F_{x'4} \\ F_{y'4} \end{Bmatrix}_n^e = \rho t [C_p^{-1}]^T \left(\iint [N_p]^T [N_p]\, dx'\, dy'\right) [C_p^{-1}]\,\{\ddot{\delta}_p'\}$$

The mass matrix is, therefore, given by

$$[m_p']^e = \rho t [C_p^{-1}]^T \left(\iint [N_p]^T [N_p]\, dx'\, dy'\right) [C_p^{-1}] \tag{3.55}$$

If the thickness of the element is constant the in-plane mass matrix reduces to

$$[m_p'] = \frac{M_e}{3} \begin{bmatrix} \frac{1}{2} & & & & & \\ 0 & \frac{1}{2} & & \text{symmetric} & & \\ \frac{1}{4} & 0 & \frac{1}{2} & & & \\ 0 & \frac{1}{4} & 0 & \frac{1}{2} & & \\ \frac{1}{4} & 0 & \frac{1}{4} & 0 & \frac{1}{2} & \\ 0 & \frac{1}{4} & 0 & \frac{1}{4} & 0 & \frac{1}{2} \end{bmatrix} \tag{3.56}$$

where M_e = mass of the element.

The Bending Mass Matrix:

The inertia force, per unit volume, at a point due to transverse acceleration, is given by

$$F_{z'4} = -\rho \ddot{w}'$$

From eq. (3.17) through eq. (3.22a)

$$F_{z'4} = -\rho[C][C_b^{-1}]\{\delta_b'\}$$

The equivalent nodal force vector is given by

$$\{F_{z'4}\}_n^e = [m_b'] \{\ddot{\delta}_b'\}$$

where the bending mass matrix is given by

$$[m_b'] = \rho t [C_b^{-1}]^T \left(\iint [C]^T [C] \, dx' \, dy'\right) [C_b^{-1}] \tag{3.57}$$

or

$$[m_b'] = \rho t [C_b^{-1}]^T \left(\iint [CC] \, dx' \, dy'\right) [C_b^{-1}]$$

where

$$[CC] = [C]^T [C]$$

$[CC]$ is a symmetric 9 x 9 matrix given by:

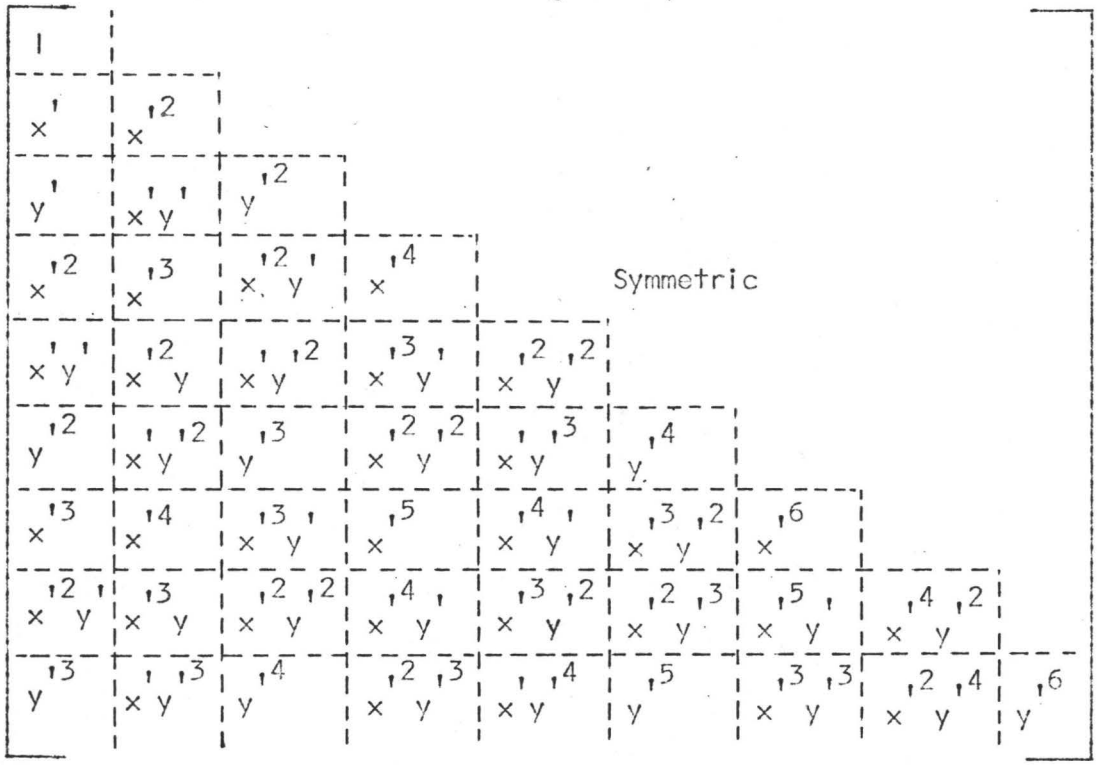

The complete mass matrix of the element is obtained by combining the in-plane and the bending mass matrices following the same procedure as for the stiffness matrices. Fictitious moment M_z, and the corresponding nodal displacement θ_z, are introduced. The complete mass matrix of the element is given by

$$[m']^e = \begin{bmatrix} m^{',11} & m^{',12} & m^{',13} \\ m^{',21} & m^{',22} & m^{',23} \\ m^{',31} & m^{',32} & m^{',33} \end{bmatrix}$$

where

$$[m^{',\gamma s}] = \begin{bmatrix} m_p^{',\gamma s} & 0 & 0 \\ 0 & m_b^{',\gamma s} & 0 \\ 0 & 0 & 0 \end{bmatrix}$$

$[m_p^{',\gamma s}]$ and $[m_b^{',\gamma s}]$ being the 2 x 2 and 3 x 3 sub-matrices of the in-plane and the bending mass matrices respectively.

The element mass matrix $[m']^e$ in the local co-ordinates is transformed to the global co-ordinates by the relation

$$[m]^e = [T]^T [m']^e [T]$$

$[T]$ being the matrix of transformation defined by eq. (3.30b).

The mass matrix for the complete blade, $[M]^s$, is obtained by assembling the element mass matrices following the same procedure as for the stiffness matrices.

CHAPTER 4

RESULTS AND DISCUSSION

Results have been obtained for the deflection of the blade with speed, and variation of the natural frequencies with speed. The calculations have been made for a fan with the following blade parameters:

i) Blade thickness = 0.020"

ii) Blade width = 3.0"

iii) Length of the blade along the post = 6.0"

iv) Post angle = 60°

v) Radial distance of the lower edge of the blade at the post = 2.625"

vi) Radius of curvature of the blade = 12.0"

vii) Material of the blade = Steel ($E = 30 \times 10^6$)

The deflection function chosen for the present analysis has already been successfully used by Rawtani (14) who has also tested it in detail for convergence and accuracy, for static and dynamic analysis.

4.1 Deflection

The flow chart for the computer programme, for the calculation of the deflected position of the blade at any speed, is attached as Appendix V.

The program uses small speed increments during which the deflection of the blade is assumed to be linear. The results have been obtained by

taking a speed increment of 100 rpm for every iteration.

The effect of the mesh size on the results is indicated in Table I where deflection at 500 rpm with different mesh sizes is given. The results show that even coarse mesh size (2 x 2 or 3 x 3) gives fairly good result. To obtain the deflected shape of the blade it is necessary to have at least 4 sub-divisions along the width of the blade. The number of sub-divisions along the length depends upon the number of different sections of the blade where deflected shape is of interest - 2 length-wise sub-divisions would give deflected shape of the top edge, middle section and bottom edge of the blade.

The results for the deflection curve have been obtained with length-wise sub-division = 2 and breadth-size sub-divisions = 5 (i.e. mesh size = 2 x 5 with 15 nodes). Figs. 4.1, 4.2, & 4.3 show the deflected shape of the top-edge, middle section and bottom-edge of the blade, respectively.

The scale on one side of the graphs has been magnified to show the variation of the curvature qualitatively. The axis of rotation has also been indicated. As expected, the blade deflects away from the axis of rotation.

TABLE I

DEFLECTION OF THE BLADE TIP AT 500 rpm

Mesh Size (NL x NB)	Number of Nodes	Degree of Freedom	Deflection (inches)
2 x 2	6	33	0.0247
3 x 3	12	68	0.0251
4 x 4	20	115	0.0253
4 x 3	15	85	0.0240
2 x 5	15	87	0.0261

NL = Length-wise sub-divisions

NB = Breadth-wise sub-divisions

The results show that the tip of the blade at the top-edge deflects by 0.324" at 5000 rpm. Also, as expected, the top edge of the blade deflects more than the bottom edge. The difference between the deflections of tip at the top-edge and the bottom edge is 0.030" at 5000 rpm.

4.2 Natural Frequencies

The flow chart for the computer programme, for calculating the natural frequencies at any speed, is attached as Appendix VI. This program calculates the natural frequencies at any particular speed. The positions of the nodes at any speed, are fed-in as data to the program.

The effect of the mesh size on the natural frequencies at zero speed is shown in Table 2.

The results of the deflection for 2 x 5 mesh from the earlier program, were used to evaluate the natural frequencies. The mesh size was increased to 4 x 5 by generating the co-ordinates of intermediate nodes by linear interpolation. This was necessary to economize on the computer time.

The first five natural frequencies of the blade up to 5000 rpm, in steps of 1000 rpm, have been computed and shown in Table 3. The variation of the natural frequencies with speed is shown graphically in Fig. 4.4.

The mode shapes at zero speed are shown in Fig. 4.5. The modes of vibration remain unchanged up to 5000 rpm.

TABLE 2

FIRST FIVE NATURAL FREQUENCIES AT ZERO SPEED

Mesh Size (NL x NB)	2 x 2	2 x 5	3 x 5	4 x 5
Natural Frequencies (cps)	56.35	44.99	46.87	50.10
	98.91	99.69	99.55	97.93
	288.47	217.43	291.39	314.87
	396.36	229.47	365.75	382.25
	423.64	229.35	441.79	487.00

The first and the third modes are bending modes while the second mode is torsional. The fourth and the fifth modes are mixed.

The effect of vibration in the centrifugal force field has also been studied. As discussed in Chapter 3, the inertia forces at any point on the blade during vibration consist of three components - (F_{x2}, F_{y2}, F_{z2}), (F_{x3}, F_{y3}, F_{z3}) and (F_{x4}, F_{y4}, F_{z4}). The components F_{x3}, F_{y3}, F_{z3} are due to Coriolis forces proportional to velocity and lead to a matrix similar to damping matrix. These forces, thus, create phase differences and have been neglected in the present study. The components F_{x2}, F_{y2}, and F_{z2} are proportional to displacement and the square of the rotational speed and affect the stiffness matrix. The components F_{x4}, F_{y4}, and F_{z4} are proportional only to acceleration and lead to mass matrix.

To study the effect of components F_{x2}, F_{y2}, and F_{z2}, of the inertial forces, the natural frequencies were also calculated without taking into account the stiffness matrix due to these forces (i.e. the "stiffness correction matrix", K_{sc}). The results are given in Table 4. It is observed that the effect of the "stiffness correction matrix" is to reduce the natural frequencies. The amount of reduction is small and increases with speed - at 5000 rpm the first frequency is reduced by 1.5% and the second by 1.04% and others by lesser amounts. The modes of vibration remain unaffected.

TABLE 3

FIRST FIVE NATURAL FREQUENCIES (cps) AT DIFFERENT SPEEDS

Speed (rpm) NO	0	1000	2000	3000	4000	5000
1	50.10	118.13	156.84	186.19	211.21	232.18
2	97.93	150.98	191.97	225.32	254.56	277.37
3	314.87	430.56	511.63	578.12	637.73	676.81
4	382.25	475.09	546.86	609.60	669.78	721.82
5	487.00	539.64	590.68	638.27	683.90	732.39

TABLE 4

NATURAL FREQUENCIES (CPS) WITH AND WITHOUT MATRIX K_{SC}

SPEED (rpm)	1000		2000		3000		4000		5000	
No.	Without K_{SC}		Without K_{SC}		Without K_{SC}		Without K_{SC}		Without K_{SC}	
1	118.52	118.13	157.91	156.84	188.07	186.19	213.9	211.21	235.7	232.18
2	151.28	150.98	192.84	191.97	226.87	225.32	256.8	254.56	280.3	277.37
3	430.67	430.56	512.01	511.63	578.84	578.12	638.8	637.73	678.4	676.81
4	475.20	475.09	547.22	546.86	610.29	609.60	670.8	669.78	723.3	721.82
5	539.74	539.64	591.04	590.68	638.99	638.27	685.0	683.90	733.9	732.39

4.3 Discussion

1) The natural frequencies increase with the speed of rotation. This is expected since the stresses in the blade make it stiffer, and the stresses increase with speed.

2) The results have been obtained by assuming the blade to be fixed as a cantilever along the post. As discussed in Chapter 3, Section 3.3, this assumption makes the blade less stiff than it actually is, since the effect of the "lip" under the blade is neglected. The program can be modified to suit the "variable boundary condition" (the condition (b) in Sec. 3.3). The outline of this formulation is discussed in Appendix VII.

3) The results reported here are for one configuration of the blade. The deflection and vibration data can be obtained for different blade parameters (angle of the post, blade thickness and other dimensions etc.) by suitably changing these parameters in the program. This information can be useful at the design stage.

FIGURES, REFERENCES AND APPENDICES

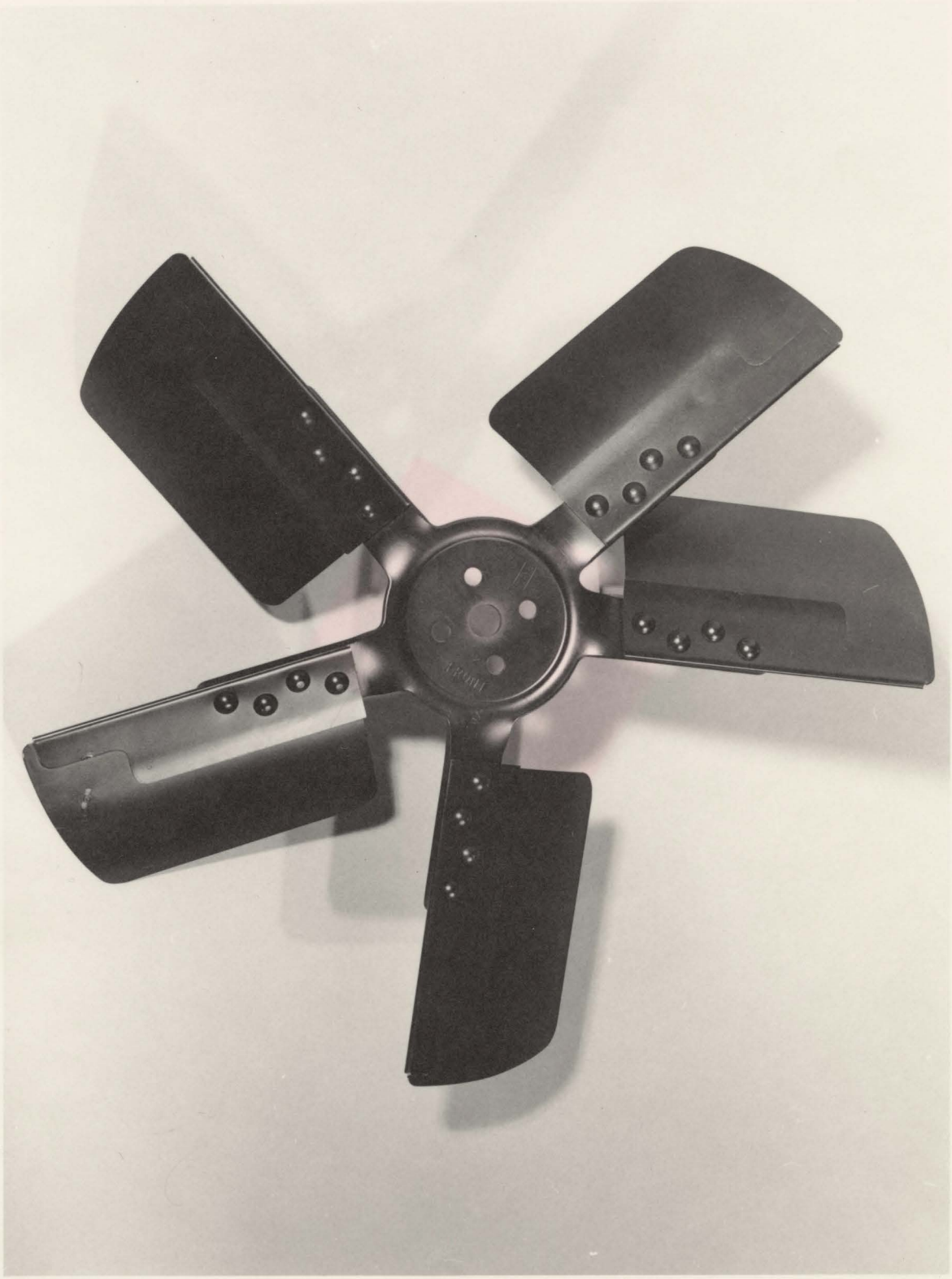

PLATE 1

Influence of cylinder (cooling water) temperature upon the average loss of pressure

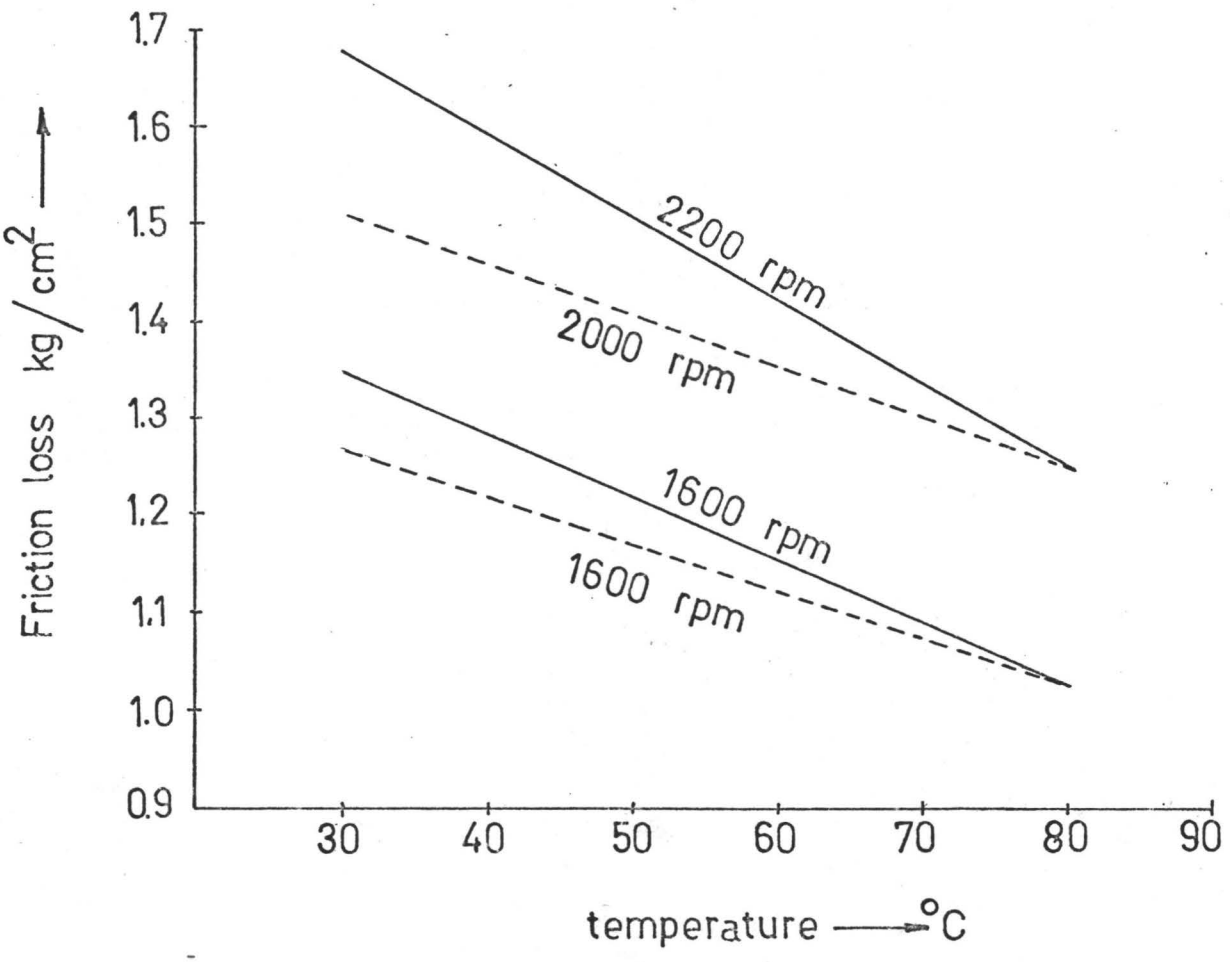

——— 12 cylinder engine, compression ratio 5.3:1, 114.3 mm bore, 152.4 mm stroke

– – – – – 8 cylinder engine, compression ratio 5.4:1, 140 mm bore, 150 mm stroke

(Ref. Mackerle [2])

FIG 1.1

Characteristics of temperature sensitive clutch and fan

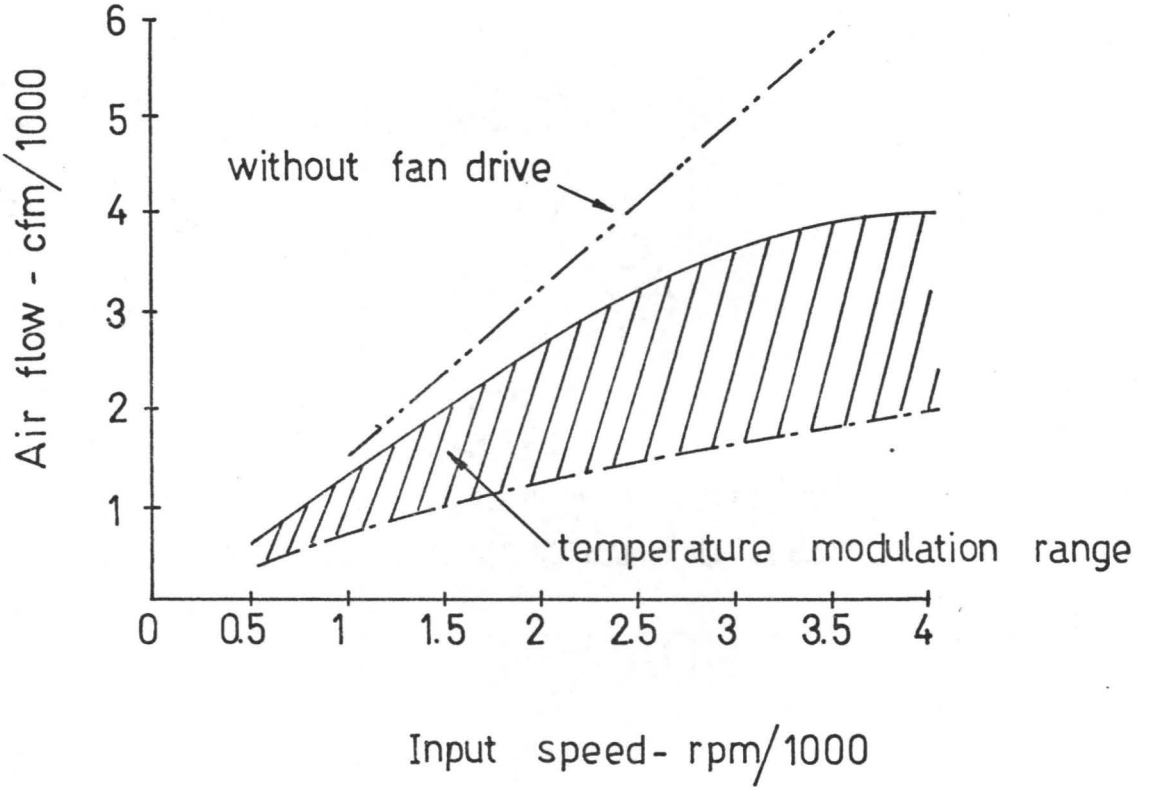

(REF. CASSIDY & WHITE [1])

FIG 1.2

Characteristics of temperature sensitive viscous clutch & fan

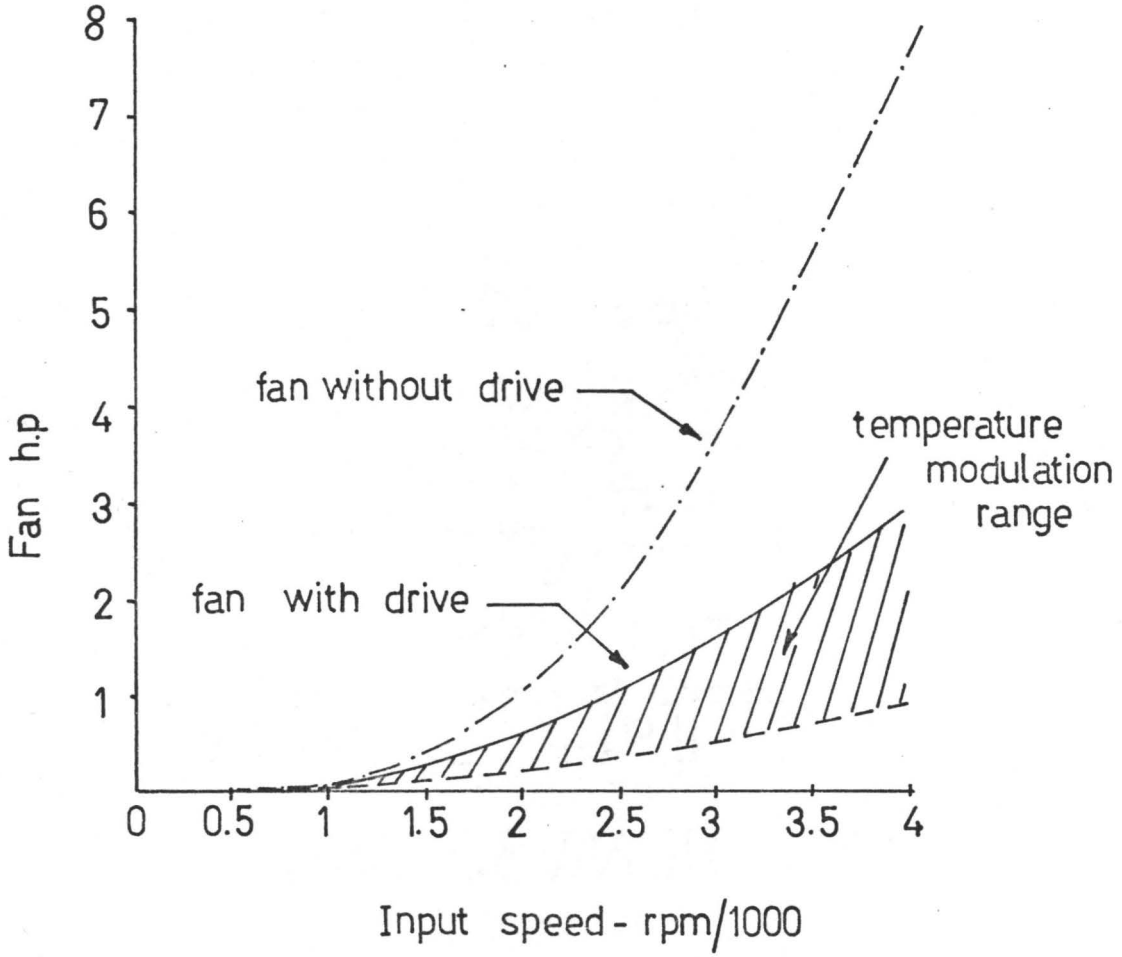

(REF. CASSIDY &WHITE [1])

FIG 1.3

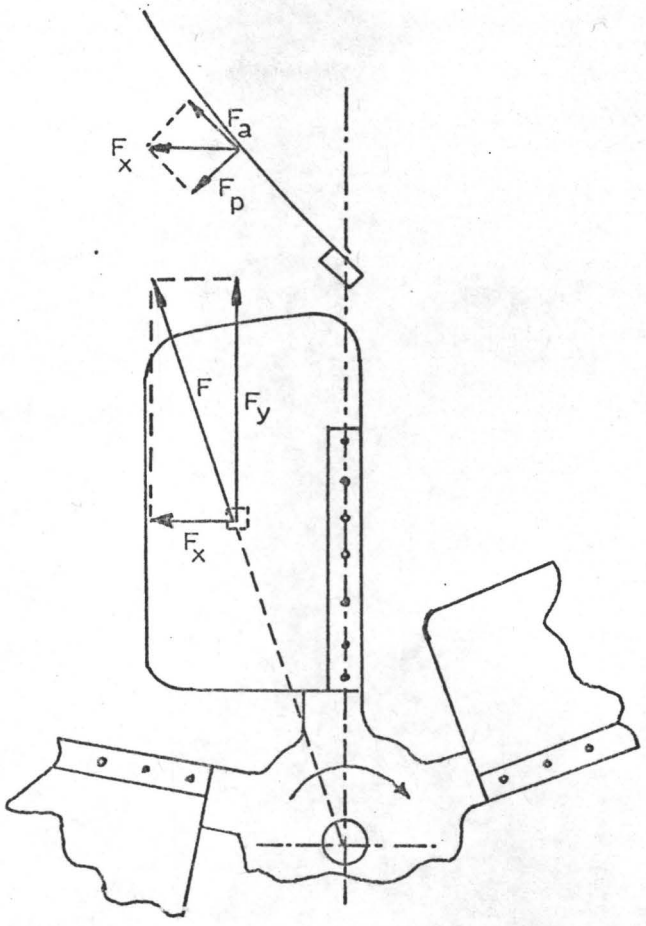

Principle of flex fan

FIG 1.4

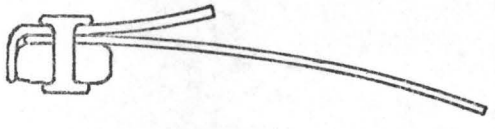

Detail of the rivetted edge

FIG 1.5

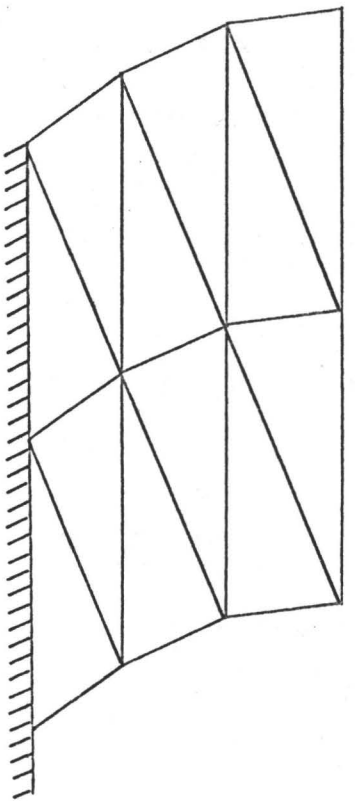

Idealisation of the fan blade

FIG 3.1

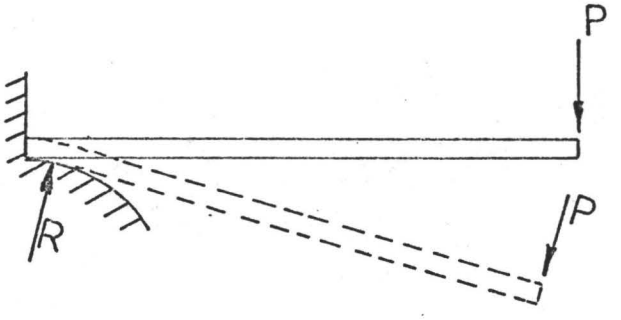

FIG 3.2

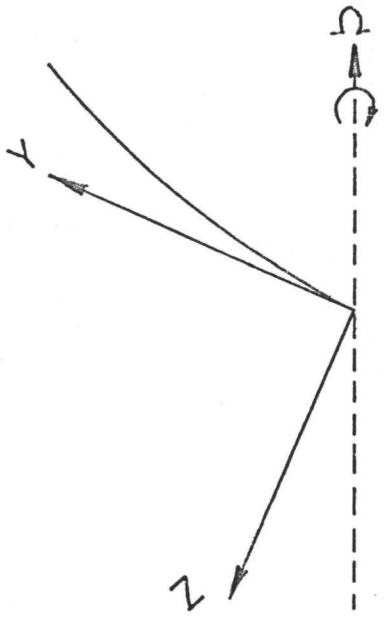

Global co-ordinates

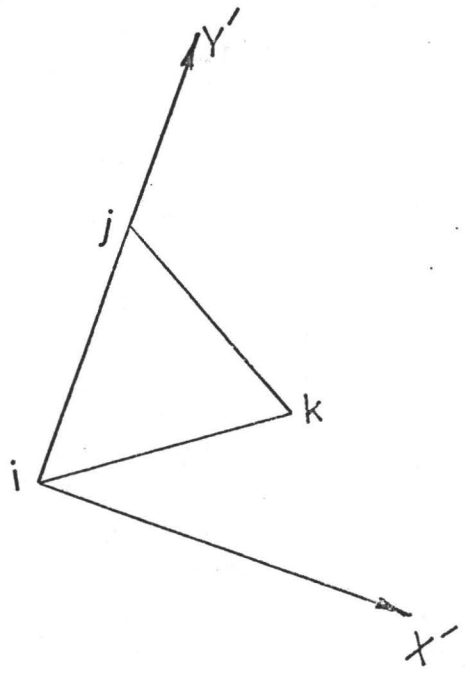

Local co-ordinates for an element

FIG 3.3

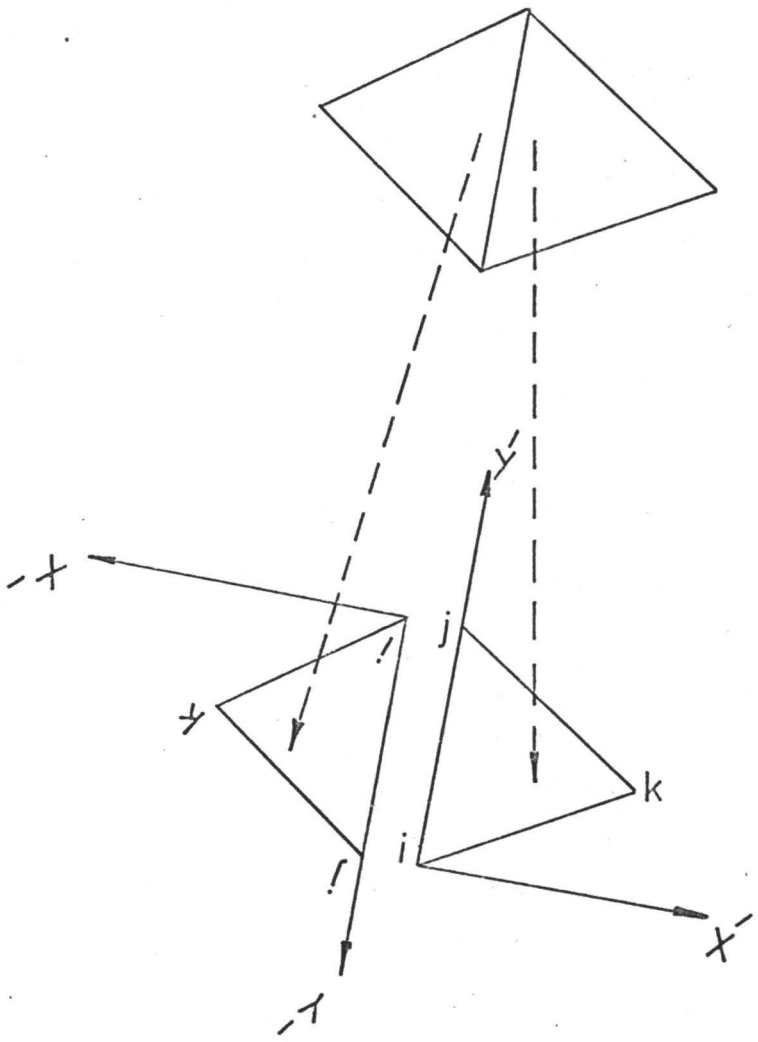

Local co-ordinates for two adjacent elements

FIG 3.4

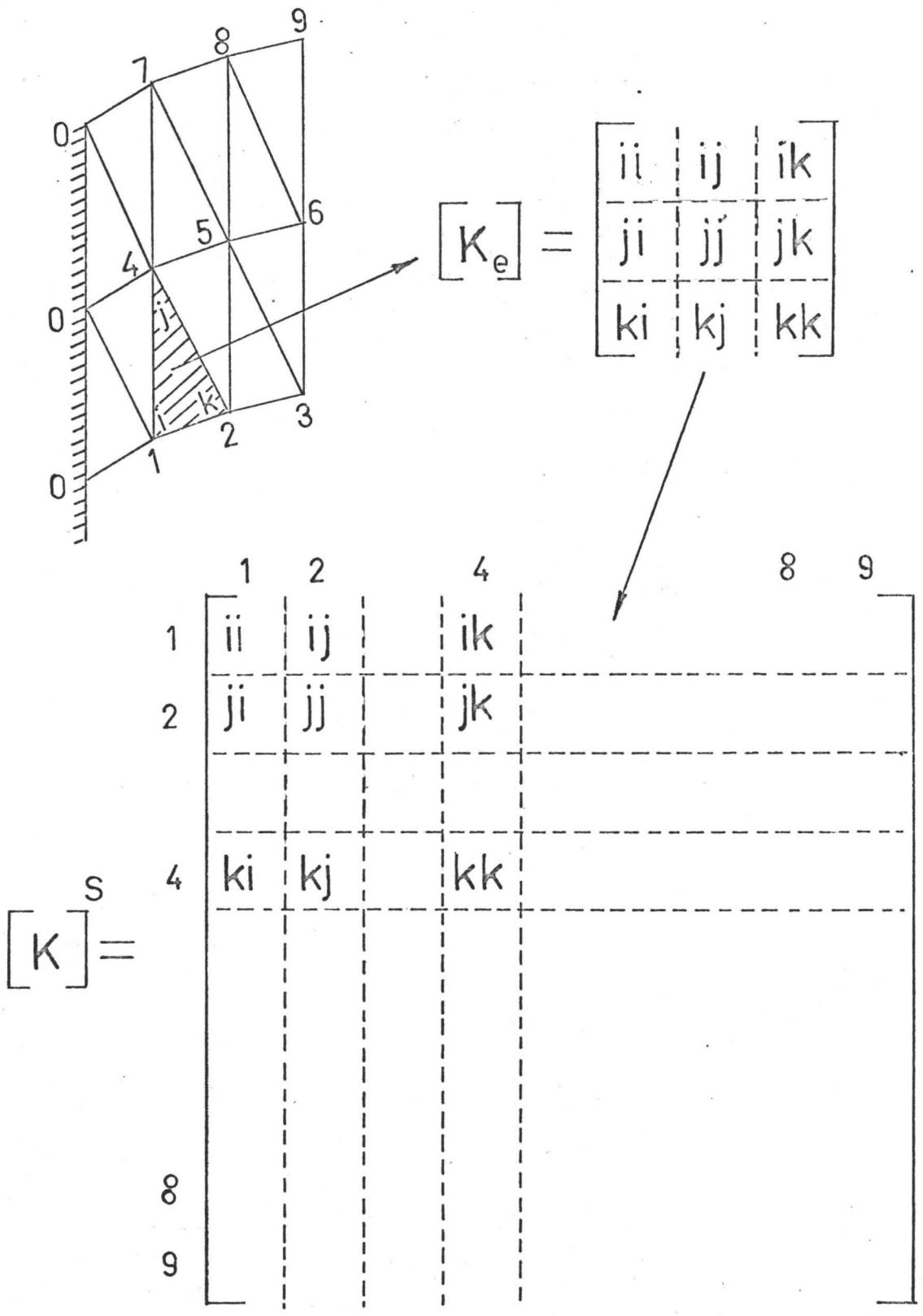

An illustration of the method of assembling the element stiffness matrix in system stiffness matrix

FIG 3.5

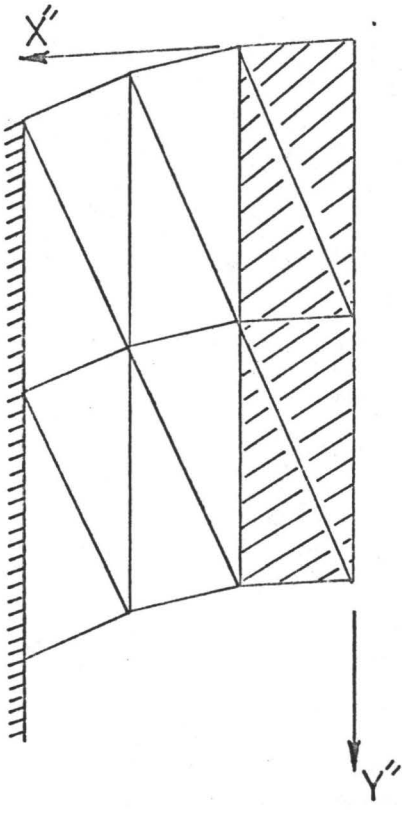

Axis $\bar{X}''$-Y'' for transformation of edge nodes

FIG 3.6

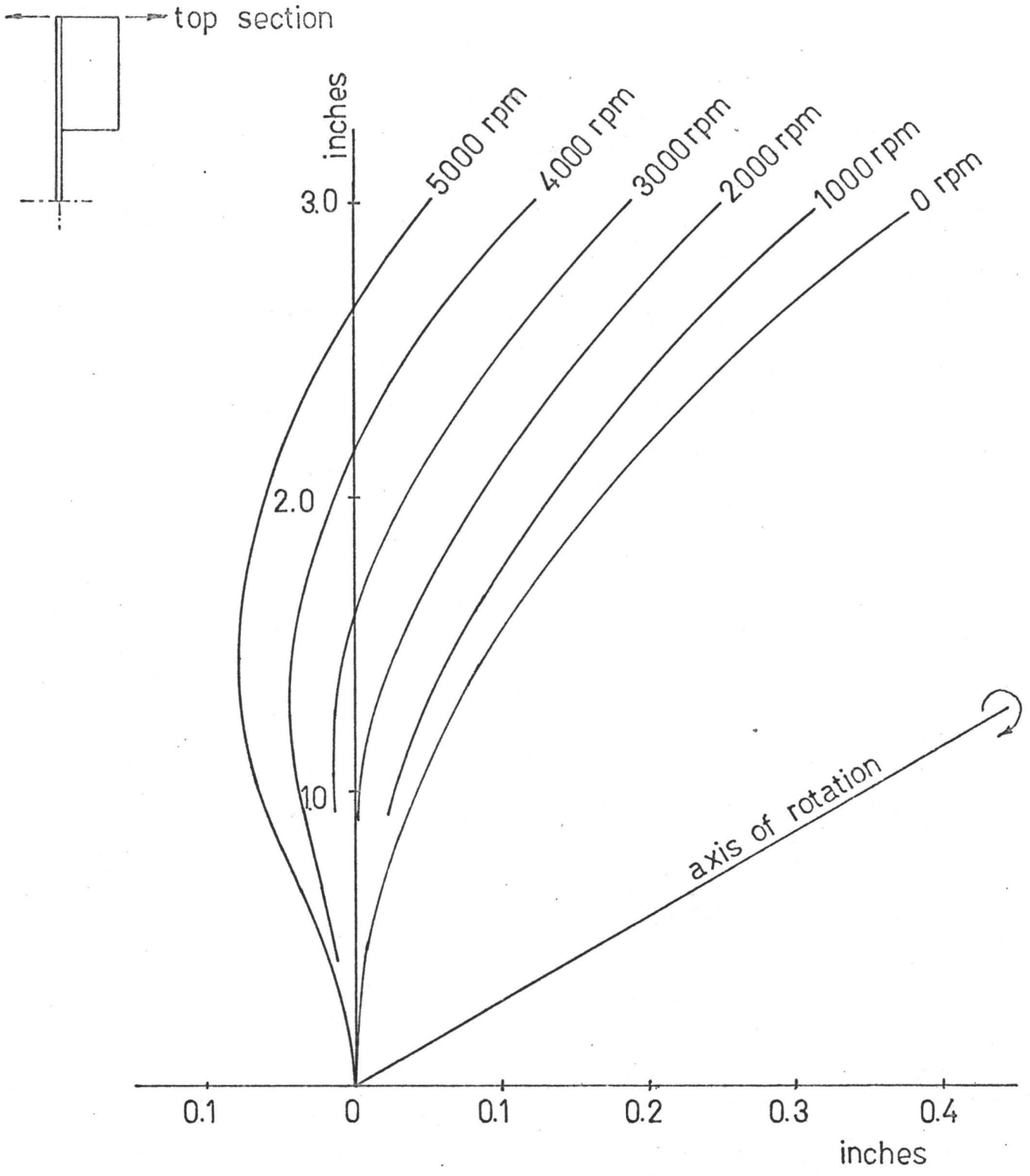

Deflected shape of the blade at the top section

FIG 4.1

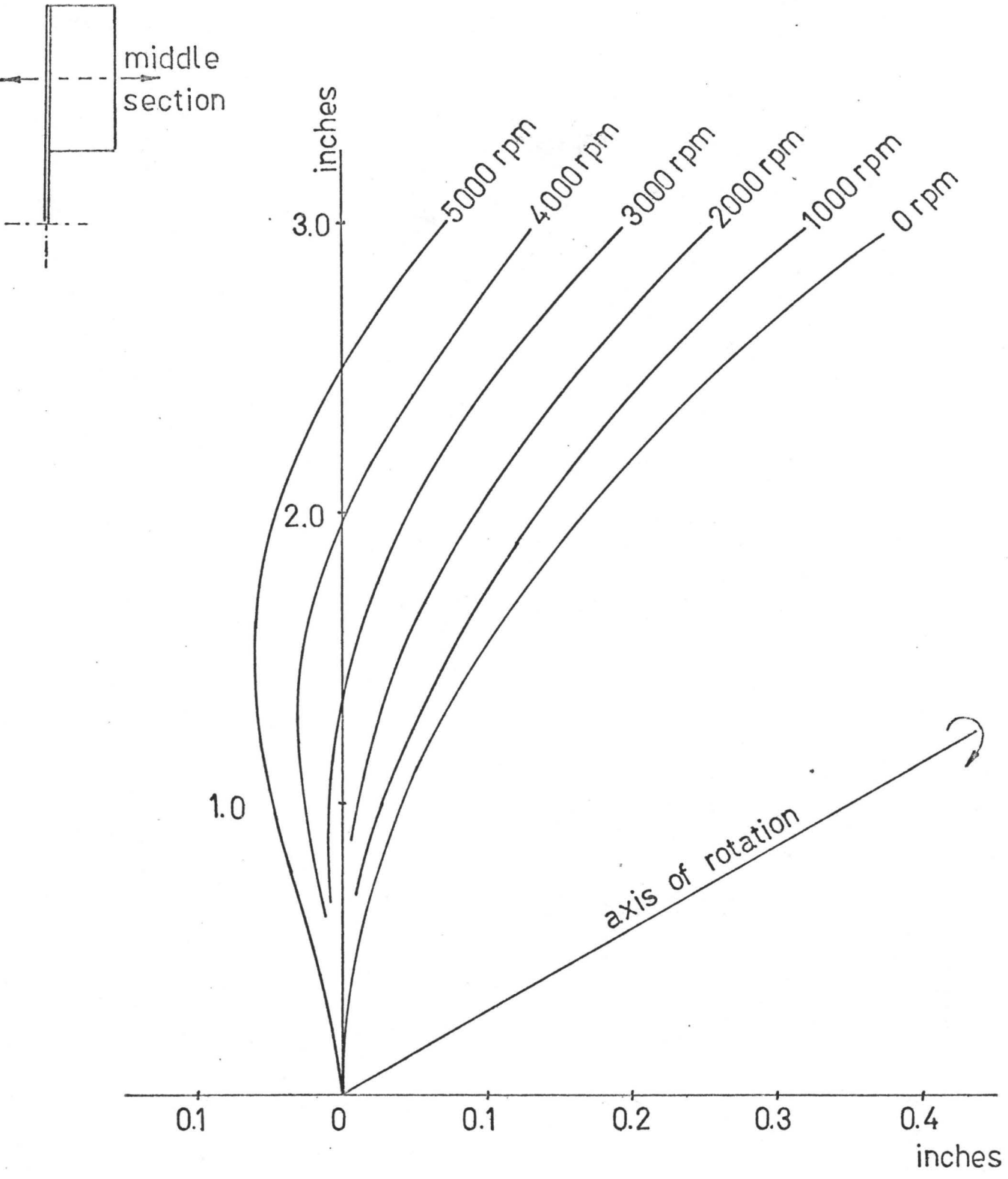

Deflected shape of the blade at the middle section

FIG 4.2

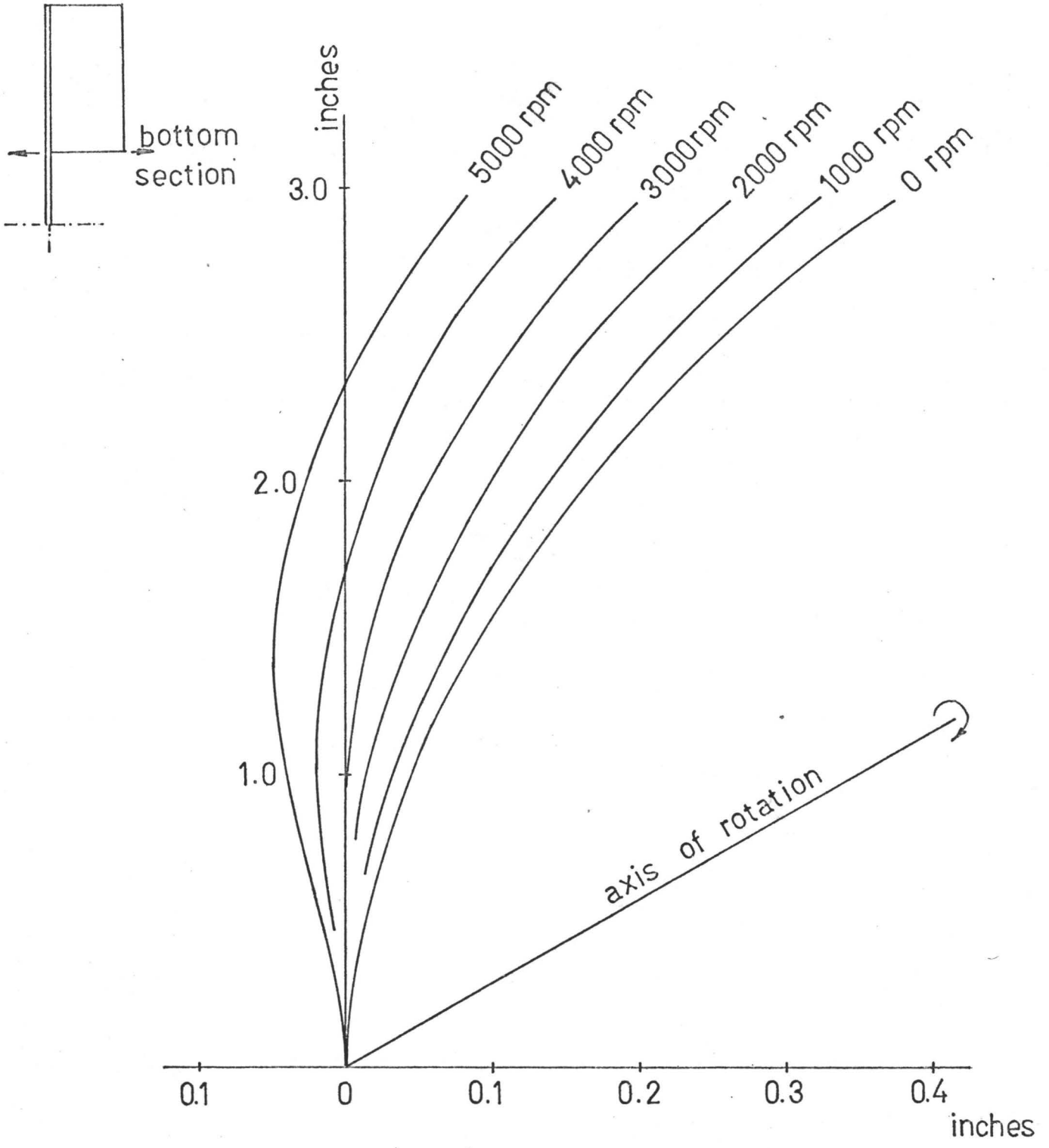

Deflected shape of the blade at the bottom section

FIG 4.3

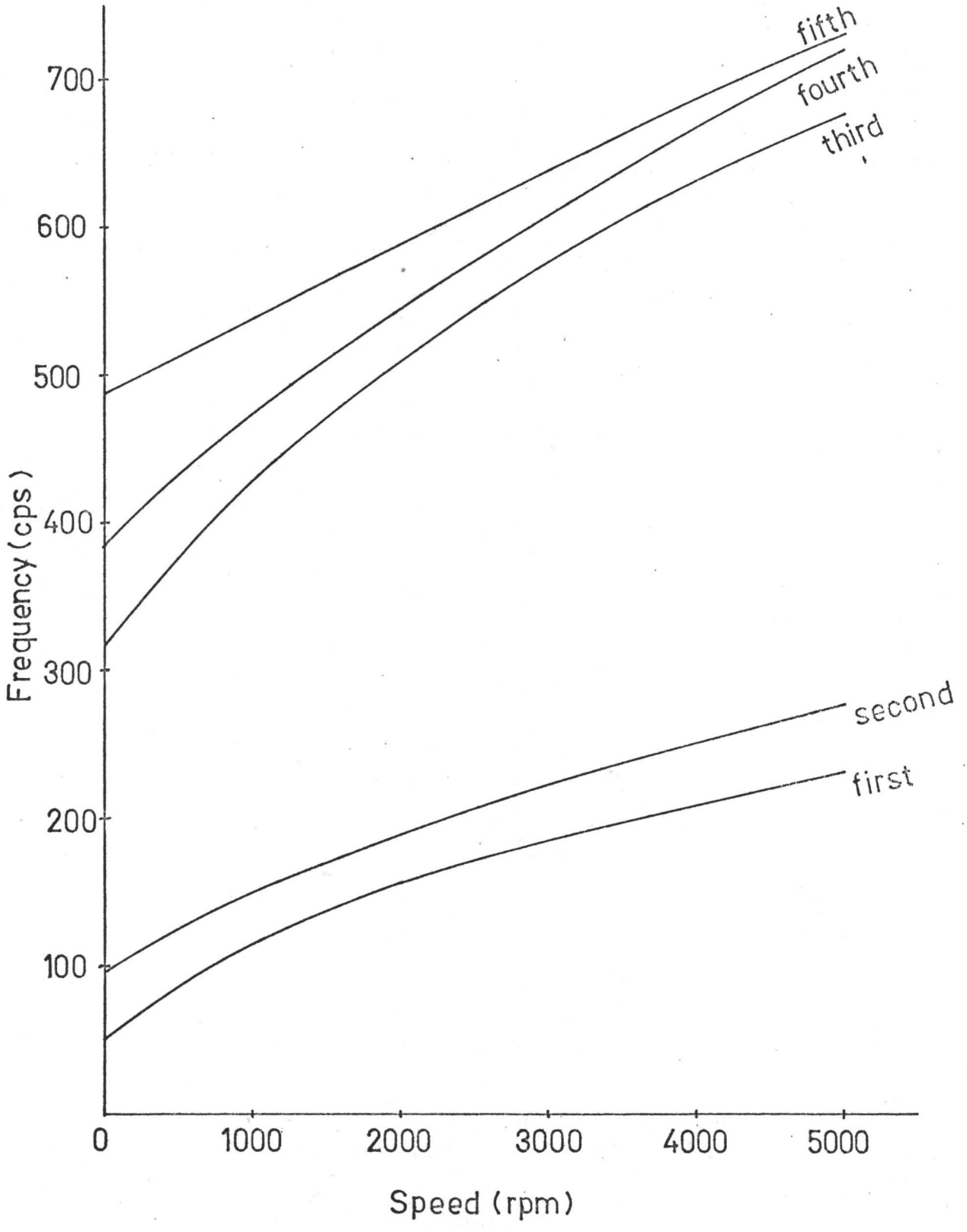

Variation of the natural frequencies with speed

FIG 4.4

MODE SHAPES

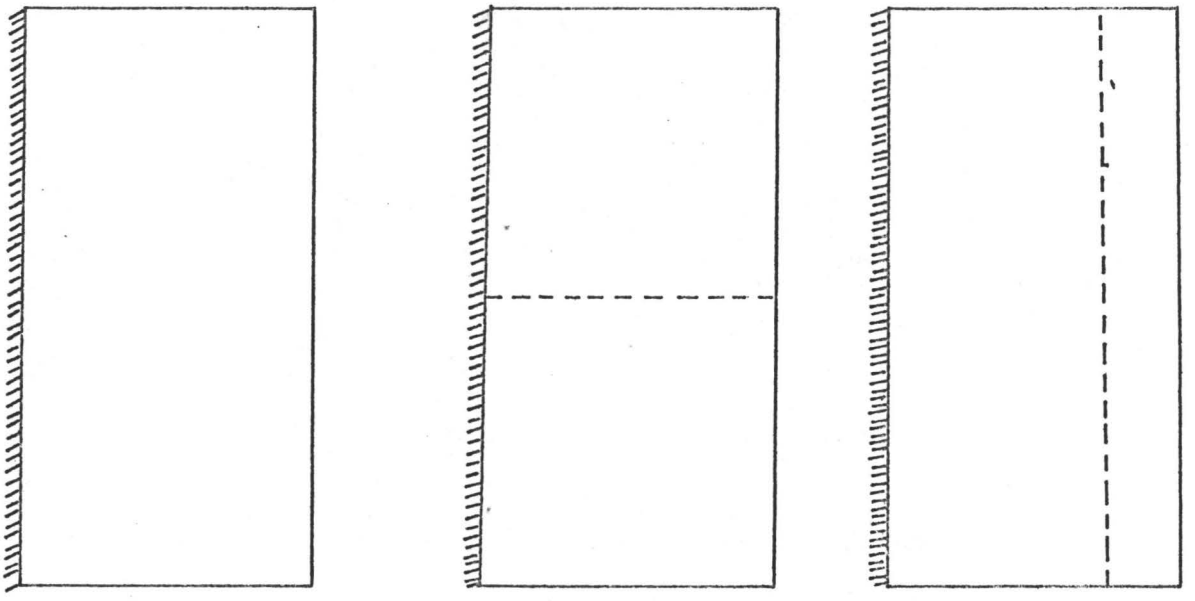

first
(bending)

second
(torsion)

third
(bending)

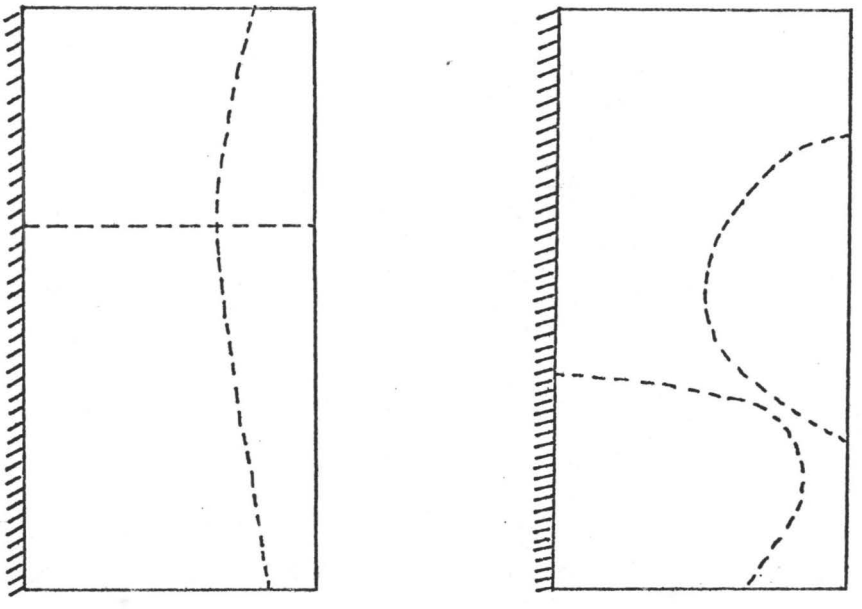

fourth
(mixed)

fifth
(mixed)

FIG 4.5

REFERENCES

1. Cassidy, R.L. & White, T.Z.,
"The Ford Flex Fan"
SAE Transactions, 1966.

2. Julius Mackerle,
"Air-cooled Motor Engines",
Cleaver-Hume Press Ltd. London (1961).

3. Brabetz, J.C.,
"Engines Like to be Warm",
SAE Journal (Jan.1965).

4. Paton, C.R.,
Patent No. 2,032,224.
United States Patent Office, Feb. 25, 1936.

5. Senn, J.A.,
Patent No. 2,442,783.
United States Patent Office, June 8, 1948.

6. Posh, R.C.,
Patent No. 666,465. Issued July 9, 1963.
Canadian Patent granted to American Metal Products Co., Detroit, U.S.A.

7. Timoshenko, S.P. & Young, D.H.,
"Theory of Structures",
2nd ed., 1965, McGraw-Hill.

8. M.J. Turner, R.W. Clough, H.C. Martin & L.J. Topp,
"Stiffness and Deflection Analysis of Complex Structures",
J. Aero. Sci., 23, pp 805-23, 1956.

9. Clough, R.W.,
"The Finite Element in Plane Stress Analysis",
Proc. 2nd A.S.C.E. Conference on Electronic Computation,
Pittsburgh, Pa., Sept. 1960.

10. Fraeijs de Veubeke, B.,
"Displacement and Equilibrium Models in the Finite Element Method",
Chpt. 9 of Stress Analysis, ed. O.C. Zienkiewicz and G.S. Hollister,
Wiley, 1965.

11. Argyris, J.H.,
"Triangular Elements with Linearly Varying Strain for the Matrix Displacement Method",
J. Roy. Aero. Soc. Tech. Note, 69, pp 711-13, Oct. 1965.

12. Melosh, R.J.,
"A Stiffness Matrix for the Analysis of Thin Plates in Bending",
J. Aerospace Sci., 28: 34-42, 64 (1961).

13. Bogner, F.K., Fox, R.L. & Schmit, L.A. Jr.,
"The Generation of Inter Element Compatible Stiffness and Mass Matrices by the Use of Interpolation Formulas"
(Addendum to) Matrix Methods in Structural Mechanics, AFFDL-TR-66-80, Wright Patterson Air Force Base, Ohio.

14. Butlin, G.A. & Leckie, F.A.,
"A Study of Finite Elements Applied to Plate Flexure",
Symposium Papers, Numerical Methods for Vibration Problems, Vol. 3, 1966, University of Southampton.

15. Mason V.,
"Rectangular Finite Elements for Analysis of Plate Vibrations:,
Journal of Sound & Vibration, Vol. 7, 1968.

16. Tocher, J.L.
"Analysis of Plate Bending Using Triangular Elements",
Ph.D Dissertation, Civil Engineering Dept., University of California, Berkeley, 1962.

17. Gallaghar, R.H.,
"The Development and Evaluation of Methods of Thin Shell Structural Analysis",
Ph.D Thesis, State University of New York (1966).

18. Rawtani, S.,
"Vibration Analysis of Rotating Low Aspect Ratio Blades Idealized as Pretwisted Cantilever Plates",
Ph.D Thesis, McMaster University, Ontario.

19. Clough, R.W. & Tocher, J.L.,
"Finite Element Stiffness Matrices for the Analysis of Plate Bending",
Proc. Conf.,Matrix Methods Struct. Mech., Wright Patterson Air Force Base, Ohio, Oct. 26-28, 1965, AFFDL-TR-66-80, 1966.

20. Bazeley, G.P., Cheung, Y.K., Irons, B.M., Zienkiewicz, O.C.,
"Triangular Elements in Plate Bending: Conforming and Non-conforming Solutions",
Proc. Conf., Matrix Methods in Struct. Mech., Wright-Patterson Air Force Base, Ohio, 1965, AFFDL-TR-66-80, 1966.

21. Gallagher, R.H., Gellatly, R.A., Padlog, J., & Millet, R.H.,
"A Discrete Element Procedure for Thin-Shell Instability Analysis",
J. Am. Inst. Aero. Astron., 5: 138-145 (1967).

22. Melosh, R.J.,
"Basis for Derivation of Matrices for the Direct Stiffness Method",
J. Am. Inst. Aero. Astron., 1: 1631-1637 (1963).

23. Zienkiewicz, O.C. & Cheung, Y.K.,
"The Finite Element Method for Analysis of Elastic Isotropic and Orthotropic Slabs",
Proc. Inst. Civ. Eng., 28, pp 471-88, 1964.

24. Dane, D.J.,
"Parallelogram Element in the Solution of Rhombic Cantilever Plate Problems",
J. of Strain Analysis, 3, 1966.

25. Argyris, J.H.,
"Continua and Discontinua",
Proc. Conf. Matrix Methods in Struct. Mech., Wright-Patterson Air Force Base, Ohio, 1965.

26. Cowper, G.R., Kosko, E., Lindberg, G.M., & Olson, M.D.,
"A High Precision Triangular Plate-bending Element",
National Research Council of Canada, Aeronautical Report LR-514, Dec. 1968.

27. Bill Kolbein,
"A Refined Triangular Plate Bending Finite Element",
International Journal for Numerical Methods in Engineering, Vol. 1, 101-122 (1969).

28. Jones, R.E., & Strome, D.R.,
"A Survey of Analysis of Shells by the Displacement Method",
Proc. Conf., Matrix Methods Struct. Mech., Wright-Patterson Air Force Base, Ohio, 1965, AFFDL-TR-66-80 (1966).

29. Zienkiewicz, O.C. & Cheung, Y.K.,
"The Finite Element Method in Structural and Continuum Mechanics",
McGraw Hill (1967).

30. Clough, R.W. & Johnson, R.R.,
"A Finite Element Approximation for the Analysis of Thin Shells",
Int. J. of Solids Structures, 4, 43-60 (1968).

31. Bogner, F.K., Fox, R.L., & Schmit, L.A.,
"A Cylindrical Shell Discrete Element",
AIAA Journal, 5, 745-750 (1967).

32. Cantin, G., & Clough, R.W.,
"A Curved Cylindrical Shell Finite Element",
AIAA Journal, Vol. 6, 1057-1062, (1968).

33. Olson, M.D. & Lindberg, G.M.,
"Vibration Analysis of Cantilevered Curved Plates Using a New Cylindrical Shell Finite Element",
Proc. 2 nd. Conf., Matrix Methods in Structural Mechanics,
Wright-Patterson Air Force Base, Ohio, 1968.

34. Connor, J.J. & Brebbia, C.,
"Stiffness Matrix for Shallow Rectangular Shell Element",
J. Eng. Mech. Div., Amer. Soc. Civ. Engrs., 93, EMS, 43-65 (1967).

35. Utku, S. & Melosh, R.J.,
"Behaviour of Triangular Shell Element Stiffness Matrices Associated with Polyhedral Displacement Distributions",
AIAA Journal Vol. 6, 374-376 (1968).

36. Strickland, G.E. & Loden, W.A.,
"A Doubly Curved Triangular Shell Element",
Proc. 2nd Conf., Matrix Methods Struct. Mech., Wright-Patterson Air Force Base, Ohio (1968).

37. Bounes, G., Dhatt, G., Giroux, Y.M. & Robichand, L.P.,
"Curved Triangular Elements for the Analysis of Shells",
Proc. 2nd Conf.,Matrix Methods Struct. Mech., Wright-Patterson Air Force Base, Ohio, (1968).

38. Cowper, G.R., Lindberg, G.M., & Olson, H.D.,
"A Shallow Shell Finite Element of Triangular Shape",
Int. J. of Solids & Structures, Vol. 6, 1133-1156, 1970.

39. Przemieniecki, J.S.,
"Theory of Matrix Methods in Structural Analysis",
McGraw Hill (1968).

40. Rubenstein, M.F.,
"Structural Systems-Statics, Dynamics and Stability",
Prentice-Hall Inc. (1970).

41. Timoshenko, S.P.,
"Strength of Materials - Part II",
page 59-63. D. Van Nostrand Co.

42. Kapur, K.K. & Hartz, B.J.,
"Stability of Thin Plates Using the Finite Element Method",
Proc. A.S.C.E. EM2, pp 177-95, 1966.

43. Halfman, R.L.,
"Dynamics",
Addison-Wesley Publishing Co. (1962).

APPENDIX I

ELEMENTS OF [Z] MATRIX

[Z] is a 9 x 9 symmetric matrix. Elements in the first row and the first column are zero. The other elements are as follows:

$$Z(2,2) = \sigma_{x'}$$

$$Z(3,2) = \tau_{x'y'}$$

$$Z(3,3) = \sigma_{y'}$$

$$Z(4,2) = 2x'\sigma_{x'}$$

$$Z(4,3) = 2x'\tau_{x'y'}$$

$$Z(4,4) = 4x'^{2}\sigma_{x'}$$

$$Z(5,2) = y'\sigma_{x'} + x'\tau_{x'y'}$$

$$Z(5,3) = y'\tau_{x'y'} + x'\sigma_{y'}$$

$$Z(5,4) = 2x'y'\sigma_{x'} + 2x'^{2}\tau_{x'y'}$$

$$Z(5,5) = y'^{2}\sigma_{x'} + x'^{2}\sigma_{y'} + 2x'y'\tau_{x'y'}$$

$$Z(6,2) = 2y'\tau_{x'y'}$$

$$Z(6,3) = 2y'\sigma_{y'}$$

$$Z(6,4) = 4x'y'\tau_{x'y'}$$

$$Z(6,5) = 2y'^{2}\tau_{x'y'} + 2x'y'\sigma_{y'}$$

$$Z(6,6) = 4y'^{2}\sigma_{y'}$$

$$Z(7,2) = 3x'^{2}\sigma_{x'}$$

$$Z(7,3) = 3x'^{2}\tau_{x'y'}$$

$$Z(7,4) = 6x'^{3}\sigma_{x'}$$

$$Z(7,5) = 3x'^{3}\tau_{x'y'} + 3x'^{2}y'\sigma_{x'}$$

$$Z(7,6) = 6x'^{2}y'\tau_{x'y'}$$

$$Z(7,7) = 9x'^{4}\sigma_{x'}$$

$$Z(8,2) = 2x'y'\sigma_{x'} + x'^{2}\tau_{x'y'}$$

$$Z(8,3) = 2x'y'\tau_{x'y'} + x'^{2}\sigma_{y'}$$

$$Z(8,4) = 4x'^{2}y'\sigma_{x'} + 2x'^{3}\tau_{x'y'}$$

$$Z(8,5) = 2x'y'^{2}\sigma_{x'} + x'^{3}\sigma_{y'} + 3x'^{2}y'\tau_{x'y'}$$

$$Z(8,6) = 4x'y'^{2}\tau_{x'y'} + 2x'^{2}y'\sigma_{y'}$$

$$Z(8,7) = 6x'^{3}y'\sigma_{x'} + 3x'^{4}\tau_{x'y'}$$

$$Z(8,8) = 4x'^{2}y'^{2}\sigma_{x'} + 4x'^{3}y'\tau_{x'y'} + x'^{4}\sigma_{y'}$$

$$Z(9,2) = 3y'^{2}\tau_{x'y'}$$

$$Z(9,3) = 3y'^{2}\sigma_{y'}$$

$$Z(9,4) = 6x'y'^{2}\tau_{x'y'}$$

$$Z(9,5) = 3y'^{3}\tau_{x'y'} + 3x'y'^{2}\sigma_{y'}$$

$$Z(9,6) = 6y'^{3}\sigma_{y'}$$

$$Z(9,7) = 9x'^{2}y'^{2}\tau_{x'y'}$$

$$Z(9,8) = 6x'y'^{3}\tau_{x'y'} + 3x'^{2}y'^{2}\sigma_{y'}$$

$$Z(9,9) = 9y'^{4}\sigma_{y'}$$

APPENDIX II

DERIVATION OF THE INERTIA FORCES

If xyz is a system of moving co-ordinate axis and XYZ is a system of fixed co-ordinates, the absolute acceleration of a point can be expressed as:

$$\vec{a} = \vec{a}' + \frac{d\vec{\Omega}}{dt} \times \vec{R} + 2\,\vec{\Omega} \times \vec{v}' + \vec{\Omega} \times (\vec{\Omega} \times \vec{R}) \qquad (a)$$

where

$\vec{a}$ = absolute acceleration

$\vec{a}'$ = translational acceleration with respect to xyz

$\vec{\Omega}$ = angular velocity of xyz system

$\vec{R}$ = position vector of the point in XYZ system

$\vec{v}'$ = velocity of the point relative to the xyz system

The proof for eq. (a) is given in most books on dynamics, e.g. Halfman [43] page 44-47.

This equation can be used to determine the absolute acceleration of a point P on the middle surface of the rotating blade.

Let the co-ordinates of the point P be xyz. Assume that the point moves to another position (x + u), (y + v) and (z + w) with acceleration $\ddot{u}$, $\ddot{v}$, $\ddot{w}$ and velocity $\dot{u}$, $\dot{v}$, $\dot{w}$ with respect to the xyz co-ordinate system, which is rotating with speed Ω, θ being the angle made by the blade post with the axis of rotation.

If i, j and k are unit vectors in the directions x, y & z respectively, the following vector equations can be written:

$$\vec{R} = i(x+u) + j(y+v) + k(z+w)$$

$$\vec{v}' = i\,\overset{\circ}{u} + j\,\overset{\circ}{v} + k\,\overset{\circ}{w}$$

$$\vec{a}' = i\,\overset{\circ\circ}{u} + j\,\overset{\circ\circ}{v} + k\,\overset{\circ\circ}{w} \qquad \text{(b)}$$

$$\vec{\Omega} = i\,0 + j\,\Omega\cos\theta + k(-\Omega\sin\theta)$$

Since the blade is rotating at constant speed $\frac{d\vec{\Omega}}{dt} = 0$.

Evaluating the right hand side of eq. (a):

$$2\vec{\Omega} \times \vec{v}' = \begin{vmatrix} i & j & k \\ 0 & 2\Omega\cos\theta & -2\Omega\sin\theta \\ \overset{\circ}{u} & \overset{\circ}{v} & \overset{\circ}{w} \end{vmatrix}$$

$$= i(2\Omega\,\overset{\circ}{w}\cos\theta + 2\Omega\,\overset{\circ}{v}\sin\theta) + j(-2\Omega\,\overset{\circ}{u}\sin\theta) + k(-2\Omega\,\overset{\circ}{u}\cos\theta)$$

$$\vec{\Omega} \times \vec{R} = \begin{vmatrix} i & j & k \\ 0 & \Omega\cos\theta & -\Omega\sin\theta \\ (x+u) & (y+v) & (z+w) \end{vmatrix}$$

$$= i\{(z+w)\Omega\cos\theta + \Omega(y+v)\sin\theta) + j\{-(x+u)\Omega\sin\theta\} + k\{-(x+u)\Omega\cos\theta\}$$

$$\therefore \vec{\Omega} \times (\vec{\Omega} \times \vec{R}) = \begin{vmatrix} i & j & k \\ 0 & \Omega\cos\theta & -\Omega\sin\theta \\ (z+w)\Omega\cos\theta + (y+v)\Omega\sin\theta & -(x+u)\Omega\sin\theta & -(x+u)\Omega\cos\theta \end{vmatrix}$$

$$= i\{-(x+u)\Omega^2\cos^2\theta - (x+u)\Omega^2\sin^2\theta\} + j\{-(z+w)\Omega^2\sin\theta\cos\theta - (y+v)\Omega^2\sin^2\theta\} + k\{-(z+w)\Omega^2\cos^2\theta - (y+v)\Omega^2\sin\theta\cos\theta\}$$

Thus, from eq. (a)

$$\vec{a} = i(\ddot{u} + 2\Omega\,\dot{w}\cos\theta + 2\Omega\,\dot{v}\sin\theta - (x+u)\Omega^2)$$
$$+ j(\ddot{v} - 2\Omega\,\dot{u}\sin\theta - (z+w)\Omega^2\sin\theta\cos\theta - (y+v)\Omega^2\sin^2\theta)$$
$$+ k(\ddot{w} - 2\Omega\,\dot{u}\cos\theta - (z+w)\Omega^2\cos^2\theta - (y+v)\Omega^2\sin\theta\cos\theta)$$

Inertia force, per unit volume, at the point can now be written. Using subscripts x, y and z for the respective directions:

$$F_x = \rho(x+u)\Omega^2 - 2\rho\Omega\dot{w}\cos\theta - 2\rho\Omega\dot{v}\sin\theta - \rho\ddot{u}$$

$$F_y = \rho(y+v)\Omega^2\sin^2\theta + \rho(z+w)\Omega^2\sin\theta\cos\theta + 2\Omega\dot{u}\sin\theta - \rho\ddot{v}$$

$$F_z = \rho(z+w)\Omega^2\cos^2\theta + \rho(y+v)\Omega^2\sin\theta\cos\theta + 2\Omega\dot{u}\cos\theta - \rho\ddot{w}$$

This is a general expression for the inertia forces. When there is no movement relative to the xyz co-ordinates, i.e. the blade is not vibrating, the inertia forces simply become:

$$F_x = \rho(x)\Omega^2$$

$$F_y = \rho(y)\Omega^2\sin^2\theta + \rho(z)\Omega^2\sin\theta\cos\theta$$

$$F_z = \rho(z)\Omega^2\cos^2\theta + \rho(y)\Omega^2\sin\theta\cos\theta$$

APPENDIX III

ELEMENTS OF THE MATRIX [NF]

The matrix [NF] is given by the relation

$$[NF] = [N]^T \begin{Bmatrix} F_{x'} \\ F_{y'} \\ F_{z'} \end{Bmatrix}$$

where [N] is a 3 x 15 matrix given by:

$$\left[\begin{array}{cccccc:c} 1 & x' & y' & 0 & 0 & 0 & \multirow{2}{*}{0} \\ 0 & 0 & 0 & 1 & x' & y' & \\ \hdashline \multicolumn{6}{c:}{\multirow{2}{*}{0}} & 1 \; x' \; y' \; x'^2 \; x'y' \; y'^2 \; x'^3 \; x'^2y' \; y'^3 \\ \multicolumn{6}{c:}{} & \end{array}\right]$$

[NF], therefore, is a 15 x 1 matrix.

Now

$$\begin{Bmatrix} F_{x'} \\ F_{y'} \\ F_{z'} \end{Bmatrix} = \begin{bmatrix} \ell_x & m_x & n_x \\ \ell_y & m_y & n_y \\ \ell_z & m_z & n_z \end{bmatrix} \begin{Bmatrix} F_x \\ F_y \\ F_z \end{Bmatrix}$$

where $\begin{Bmatrix} F_x \\ F_y \\ F_z \end{Bmatrix}$ is given by eq. (3.36a).

Therefore,

$$\begin{aligned} F_{x'} = \rho\Omega^2 \{ & x' (\ell_x^2 + m_x^2 \sin^2\theta + n_x^2 \cos^2\theta + 2 m_x n_x \sin\theta \cos\theta) \\ & + y' (\ell_x \ell_y + m_x m_y \sin^2\theta + m_x n_y \sin\theta \cos\theta + n_x m_y \sin\theta \cos\theta \\ & + n_x n_y \cos^2\theta) + x_i \ell_x + y_i m_x \sin^2\theta + z_i m_x \sin\theta \cos\theta \\ & + y_i n_x \sin\theta \cos\theta + z_i n_x \cos^2\theta \} \end{aligned}$$

$$F_{y'} = \rho\Omega^2\{x'(\ell_y\ell_x + m_y m_x \sin^2\theta + m_y n_x \sin\theta\cos\theta + n_y m_x \sin\theta\cos\theta + n_y n_x \cos^2\theta) + y'(\ell_y^2 + m_y^2 \sin^2\theta + m_y n_y \sin\theta\cos\theta + n_y m_y \sin\theta\cos\theta + n_y^2 \cos^2\theta) + x_i \ell_y + y_i m_y \sin^2\theta + z_i m_y \sin\theta\cos\theta + y_i n_y \sin\theta\cos\theta + z_i n_y \cos^2\theta\}$$

$$F_{z'} = \rho\Omega^2\{x'(\ell_x\ell_z + m_z m_x \sin^2\theta + m_z n_x \sin\theta\cos\theta + n_z m_x \sin\theta\cos\theta + n_z n_x \cos^2\theta) + y'(\ell_z\ell_y + m_z m_y \sin^2\theta + m_z n_y \sin\theta\cos\theta + n_z m_y \sin\theta\cos\theta + n_z n_y \cos^2\theta) + x_i \ell_z + y_i m_z \sin^2\theta + z_i m_z \sin\theta\cos\theta + y_i n_z \sin\theta\cos\theta + z_i m_z \cos^2\theta\}$$

The elements of [NF] are defined as follows:

$$NF(1) = F_{x'}$$

$$NF(2) = x' F_{x'}$$

$$NF(3) = y' F_{x'}$$

$$NF(4) = F_{y'}$$

$$NF(5) = F_{y'}$$

$$NF(6) = y' F_{y'}$$

$$NF(7) = F_{z'}$$

$$NF(8) = x' F_{z'}$$

$$NF(9) = y' F_{z'}$$

$$NF(10) = x'^2 F_{z'}$$

$$NF(11) = x' y' F_{z'}$$

$$NF(12) = y'^{2} F_{z'}$$

$$NF(13) = x'^{3} F_{z'}$$

$$NF(14) = x'^{2} y' F_{z'}$$

$$NF(15) = y'^{3} F_{z'}$$

APPENDIX IV

ELEMENTS OF THE MATRIX [NQ]

As defined in equation (3.53)

$$[NQ] = [N]^T [Q] [N]$$

where

$$[Q] = [\lambda] [R] [\lambda]^T$$

$[\lambda]$ is the matrix of direction cosines and $[R]$ is given by

$$[R] = \begin{bmatrix} 1 & 0 & 0 \\ 0 & \sin^2\theta & \sin\theta\cos\theta \\ 0 & \sin\theta\cos\theta & \cos^2\theta \end{bmatrix}$$

During computation $[\lambda]$ and $[R]$ are matrices with numerical values. Therefore, $[Q]$ can be obtained by multiplying $[\lambda] [R] [\lambda]^T$, so that

$$[Q] = \begin{bmatrix} Q_{11} & Q_{12} & Q_{13} \\ Q_{21} & Q_{22} & Q_{23} \\ Q_{31} & Q_{32} & Q_{33} \end{bmatrix}$$

is available in the computer.

Matrix $[N]$ is given by

$$[N] = \left[\begin{array}{cccccc|c} 1 & x' & y' & 0 & 0 & 0 & \\ 0 & 0 & 0 & 1 & x' & y' & 0 \\ \hline 0 & 0 & 0 & 0 & 0 & 0 & 1 \; x' \; y' \; x'^2 \; x'y' \; y'^2 \; x'^3 \; x'^2y' \; x'y'^2 \; y'^3 \end{array}\right]$$

The matrix [NQ] is given by the product $[N]^T [Q] [N]$. [NQ] is a 15 x 15 symmetric matrix. This may be partitioned into 5 x 5 sub-matrices as shown below

$$[NQ] = \begin{bmatrix} NQ_{11} & NQ_{12} & NQ_{13} \\ NQ_{21} & NQ_{22} & NQ_{23} \\ NQ_{31} & NQ_{32} & NQ_{33} \end{bmatrix}$$

The sub-matrices are defined as follows:

$$[NQ_{11}] = \begin{bmatrix} Q_{11} & & & & \\ x'Q_{11} & x'^2Q_{11} & \text{symmetric} & & \\ y'Q_{11} & x'y'Q_{11} & y'^2Q_{11} & & \\ Q_{21} & x'Q_{21} & y'Q_{21} & Q_{22} & \\ x'Q_{21} & x'^2Q_{21} & x'y'Q_{21} & x'Q_{22} & x'^2Q_{22} \end{bmatrix}$$

$$[NQ_{21}] = \begin{bmatrix} y'Q_{21} & x'y'Q_{21} & y'^2Q_{21} & y'Q_{22} & x'y'Q_{22} \\ Q_{31} & x'Q_{31} & y'Q_{31} & Q_{32} & x'Q_{32} \\ x'Q_{31} & x'^2Q_{31} & x'y'Q_{31} & x'Q_{32} & x'^2Q_{32} \\ y'Q_{31} & x'y'Q_{31} & y'^2Q_{31} & y'Q_{32} & x'y'Q_{32} \\ x'^2Q_{31} & x'^3Q_{31} & x'^2y'Q_{31} & x'^2Q_{32} & x'^3Q_{32} \end{bmatrix}$$

$$[NQ_{22}] = \begin{bmatrix} y^{,2} Q_{22} & & & & \\ y^{,} Q_{32} & Q_{33} & \text{symmetric} & & \\ x^{,} y^{,} Q_{32} & x^{,} Q_{33} & x^{,2} Q_{33} & & \\ y^{,2} Q_{32} & y^{,} Q_{33} & x^{,} y^{,} Q_{33} & y^{,2} Q_{33} & \\ x^{,2} y^{,} Q_{32} & x^{,2} Q_{33} & x^{,3} Q_{33} & x^{,2} y^{,} Q_{33} & x^{,4} Q_{33} \end{bmatrix}$$

$$[NQ_{31}] = \begin{bmatrix} x^{,} y^{,} Q_{31} & x^{,2} y^{,} Q_{31} & x^{,} y^{,2} Q_{31} & x^{,} y^{,} Q_{32} & x^{,2} y^{,} Q_{32} \\ y^{,2} Q_{31} & x^{,} y^{,2} Q_{31} & y^{,3} Q_{31} & y^{,2} Q_{32} & x^{,} y^{,2} Q_{32} \\ x^{,3} Q_{31} & x^{,4} Q_{31} & x^{,3} y^{,} Q_{31} & x^{,3} Q_{32} & x^{,4} Q_{32} \\ x^{,2} y^{,} Q_{31} & x^{,3} y^{,} Q_{31} & x^{,2} y^{,2} Q_{31} & x^{,2} y^{,} Q_{32} & x^{,3} y^{,} Q_{32} \\ y^{,3} Q_{31} & x^{,} y^{,3} Q_{31} & y^{,4} Q_{31} & y^{,3} Q_{32} & x^{,} y^{,3} Q_{32} \end{bmatrix}$$

$$[NQ_{32}] = \begin{bmatrix} x^{,} y^{,2} Q_{32} & x^{,} y^{,} Q_{33} & x^{,2} y^{,} Q_{33} & x^{,} y^{,2} Q_{33} & x^{,3} y^{,} Q_{33} \\ y^{,3} Q_{32} & y^{,2} Q_{33} & x^{,} y^{,2} Q_{33} & y^{,3} Q_{33} & x^{,2} y^{,2} Q_{33} \\ x^{,3} y^{,} Q_{32} & x^{,3} Q_{33} & x^{,4} Q_{33} & x^{,3} y^{,} Q_{33} & x^{,5} Q_{33} \\ x^{,2} y^{,2} Q_{32} & x^{,2} y^{,} Q_{33} & x^{,3} y^{,} Q_{33} & x^{,2} y^{,2} Q_{33} & x^{,4} y^{,} Q_{33} \\ y^{,4} Q_{32} & y^{,3} Q_{33} & x^{,} y^{,3} Q_{33} & y^{,4} Q_{33} & x^{,2} y^{,3} Q_{33} \end{bmatrix}$$

$$[NQ_{33}] = \begin{bmatrix} x^{,2}y^{,2}Q_{33} & & & & \\ x^{,}y^{,3}Q_{33} & y^{,4}Q_{33} & \text{symmetric} & & \\ x^{,4}y^{,}Q_{33} & x^{,3}y^{,2}Q_{33} & x^{,6}Q_{33} & & \\ x^{,3}y^{,2}Q_{33} & x^{,2}y^{,3}Q_{33} & x^{,5}y^{,}Q_{33} & x^{,4}y^{,2}Q_{33} & \\ x^{,}y^{,4}Q_{33} & y^{,5}Q_{33} & x^{,3}y^{,3}Q_{33} & x^{,2}y^{,4}Q_{33} & y^{,6}Q_{33} \end{bmatrix}$$

APPENDIX V

The flow chart for the computer programme to compute the deflections of the blade is given on the next page. The symbols used are the same as in the rest of the thesis. The FORTRAN variables used are:

SPEED = Speed of rotation of the fan

EN = Element number

SINCR = Increment in speed after each iteration

SMAX = Maximum speed up to which the deflections are to be computed.

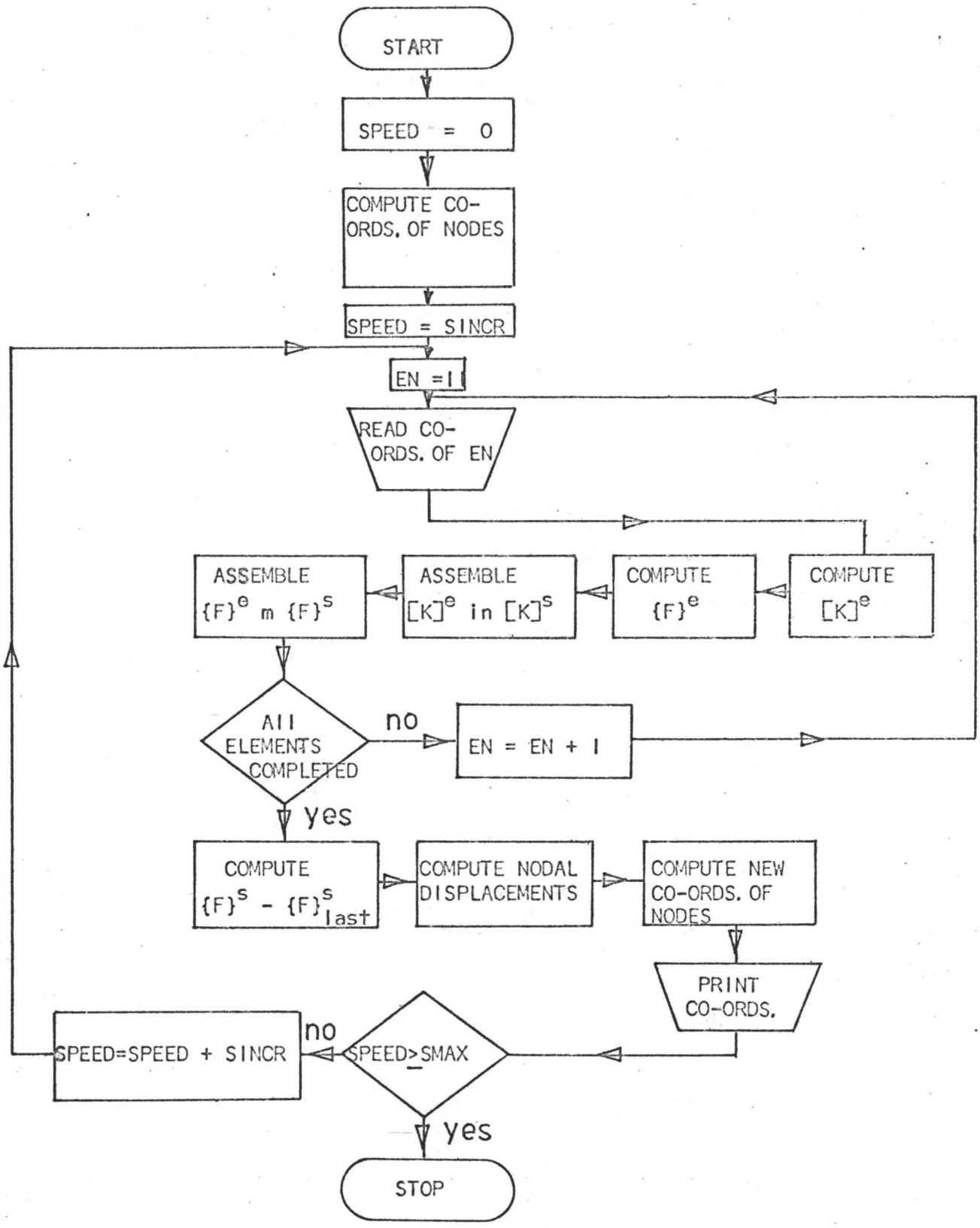

FLOW CHART FOR COMPUTATION OF DEFLECTIONS

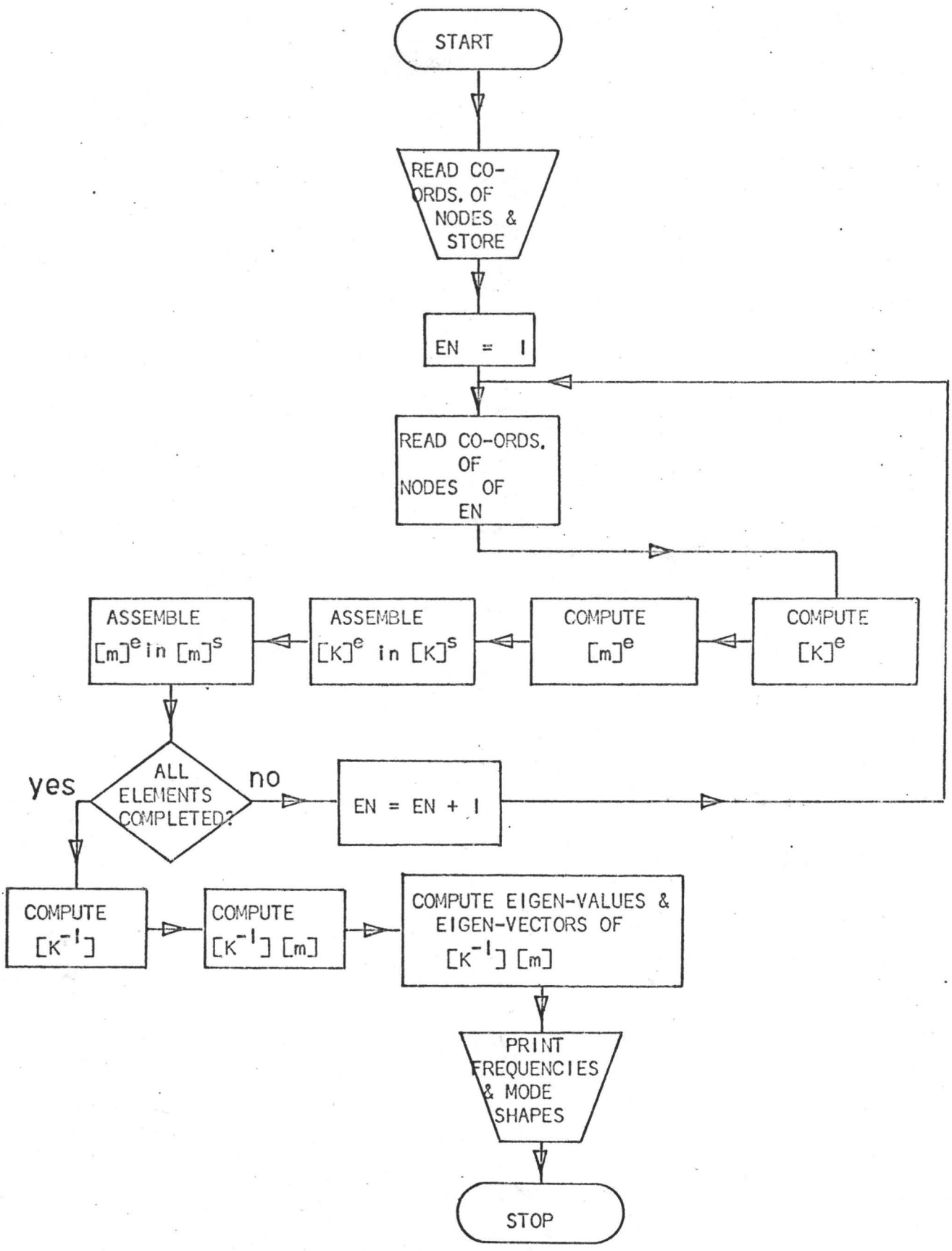

FLOW CHART FOR COMPUTATION OF NATURAL FREQUENCIES AND MODE SHAPES AT ANY SPEED (Symbols same as in Appendix V).

APPENDIX VII

MODIFICATION REQUIRED TO SUIT "VARIABLE" BOUNDARY CONDITION

As discussed in Sec. 3.3., under the "variable" boundary condition the lip is idealized as a flat surface. Any point on the lip, therefore, has Z co-ordinate = 0. The nodes on the blade surface which come in contact with this surface are assumed to be built-in from then onwards.

A large number of nodes is needed to study the effect of the lip. This necessitates a fine mesh - increasing the size of the system stiffness and mass matrices. Since the lip is small in width (3/4"), fine mesh can be used in this region and relatively coarse mesh in the rest of the blade. The present programme evaluates the co-ordinates of all the nodes at each iteration. The program can be modified such that nodes in the region of the lip are given number zero when their Z co-ordinate becomes zero, and thus are not assembled in the system stiffness and mass matrices. This results in reduction of the size of these matrices and reduced degrees of freedom for the complete structure. Since the present program uses the matrices as two-dimensional arrays, reduction in matrix size poses the problem of relocating the elements of the reduced matrix in the two-dimensional array assigned for the storing of the matrix in computer memory. This has to be carefully done before the system matrices can be operated upon.